SAND2000-2557 J

NUREG/CR-XXX
SAND~~00-XXX~~
2000-2557

Historical Case Analysis of Uranium Plume Attenuation

Manuscript Completed: September 2000
Date Published: XX 2000

Prepared by
C. F. Jove Colon, P. V. Brady,
M. D. Siegel, and E. R. Lindgren

Sandia National Laboratories
Albuquerque, NM 87185-0750

E. O'Donnell, NRC Project Manager

Prepared for
U.S. Nuclear Regulatory Commission

DISCLAIMER

Abstract

Groundwater plumes containing dissolved uranium at levels above natural background exist adjacent to uranium ore bodies at uranium mines, milling locations, and at a number of explosive test facilities. Public health concerns require that some assessment of the potential for further plume movement in the future be made. Reaction-transport models, which might conceivably be used to predict plume movement, require extensive data inputs that are often uncertain. Many of the site-specific inputs are physical parameters that can vary spatially and with time. Limitations in data availability and accuracy mean that reaction-transport predictions can rarely provide more than order-of-magnitude bounding estimates of contaminant movement in the subsurface. A more direct means for establishing the limits of contaminant transport is to examine actual plumes to determine if, collectively, they spread and attenuate in a reasonably consistent and characteristic fashion. Here a number of U plumes from ore bodies and contaminated sites were critically examined to identify characteristics of U plume movement. The magnitude of the original contaminant source, the geologic setting, and the hydrologic regime were rarely similar from site to site. Plumes also spanned a vast range of ages and no complete set of time-series plume analyses exist for a particular site. Despite the accumulated uncertainties and variabilities, the plume data set gave a clear and reasonably consistent picture of U plume behavior. Specifically, uranium plumes:

- Appear to reach steady-state, that is, they quit spreading rapidly (within a few years).
- Exceed roughly 2 km in length only in special cases e.g. where *in situ* leaching has been carried out. The majority is much smaller.
- Exhibit very similar U chemistry between sites. This implies analogous contaminant attenuation mechanisms despite their location.

CONTENTS

FIGURES

TABLES

1.0 Introduction

Uranium plumes in groundwater have been produced in the course of mining, ore processing, and weapons testing. Because of concerns about off site movement of U in groundwater, many of the sites are being actively remediated while others are being considered for remediation; most will require some long-term monitoring. Natural processes, such as sorption, mineral growth and dispersion occur in the absence of, and often in parallel with, active remediation and collectively set limits on how far a particular plume can move. To assess performance and to guide long-term monitoring, it would be useful to know what these limits are.

Conceptually, a plume of dissolved U emanating from a point source can be expected to have the highest dissolved contaminant levels near the source and progressively lower level down-gradient. In theory, the direction of maximum advance of contaminants should be parallel to the hydrologic gradient. Once the source term is removed, or treated to stop further addition of contaminant to the groundwater, e.g. with a landfill cap, dilution by fresh recharge should lead to a decrease in dissolved phase concentrations. Indeed, dilution along the leading edge of a plume alone should ultimately arrest subsequent advance of a plume. Note though that, in the absence of chemical removal mechanisms (natural or engineered), the contaminant mass in a plume is unaffected by dilution. Natural mechanisms that reduce the bioavailable mass of U in soil solutions include reversible and/or irreversible sorption and chemical transformation, e. g. reduction to less soluble forms. This natural reduction in mobile U mass would tend to hasten the cessation of plume advance. Recent work on leaking underground fuel tanks [1] suggests that if chemical processes were collectively the primary control over finite plume movement, we would expect to see similar behavior for U plume migration. For example, we might expect all U plumes to reach a similar length before halting. Knowledge of a general U plume cessation length would be useful in a public health sense as it would constitute a first step in assessing the potential impact of particular plumes on groundwater. It would also allow monitoring wells to be more effectively located for groundwater protection. We hypothesize that the natural history of U plumes is best developed by examining large numbers of individual plumes after the approach of Rice et al. [1] and resolving features of their collective advance and decay into specific chemical and physical processes.

2.0 Uranium in Soil

Feldspars in alkaline and granitic igneous rocks are the main source for much of the U present in near-surface natural environments (see table 1 for environmental concentrations of U). Transport of U dissolved from igneous source rocks typically occurs under oxidizing conditions when U is present as the uranyl ion U (VI) (UO_2^{+2})[a]. U is substantially less soluble under reducing

[a] The oxidized uranyl(VI) species will be expressed hereafter as UO_2^{++}.

conditions, when it is typically present as aqueous U $(OH)_4$.

Table 1. Typical U contents of various types rocks [2].

Rock Type	Range of Concentrations (ppm)
Igneous	
Mafic	0.1-3.5
Diorite and Quartz Diorite	0.5-12
Alkaline Intrusive	0.04-20
Sedimentary	
Shale	1-15
Black shale	3-1250
Sandstone	0.5-4
Orthoquartzite	0.2-0.6
Carbonate	0.1-10
Phosphorite	50-2500
Lignite	10-2500
Large Scale U Sources	**Average Concentration (ppm)**
High-grade U deposit	10^4-10^5
High-heat production granite	10
Continental Crust	1
Bulk Earth	2×10^{-2}

Figure 1 shows uranyl speciation under oxidizing conditions ($fO_2 = 0.2$ atm) and $pCO_2 = 10^{-3.5}$. Note the prevalence of UO_2^{++}- carbonate complexes at pH ≥ 7. In the absence of CO_2 , but at the same fO_2, uranyl-hydroxy ions predominate at pH > 5. Under nominally reducing conditions (log $fO_2 \approx$ -70 atm), 25°C, and low total U concentrations (e.g., $[U]_T < 10^{-14}$ m), U(IV) forms U-hydroxo complexes at pH ≥ 6 (Fig. 2 and table 2). However, when $[U]_T > 10^{-14}$ m, uraninite $(UO_2)_{cr}$ becomes stable.

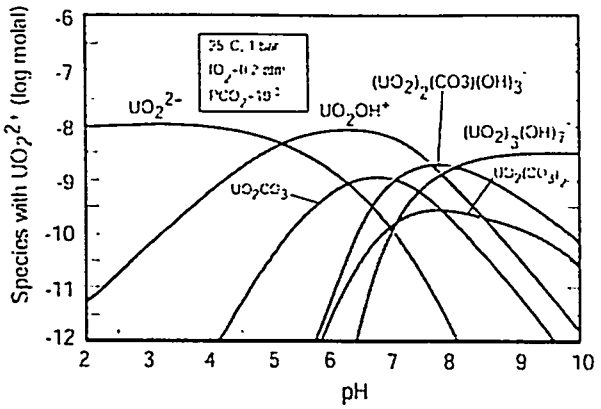

Figure 1 Uranyl speciation at 25°C and 1 bar as a function of pH under oxidizing conditions; fO_2 = 0.2 atm and $pCO_2 = 10^{-3.5}$ atm. Uranium speciation data is from the Geochemical Workbench (GWB) software package [3].

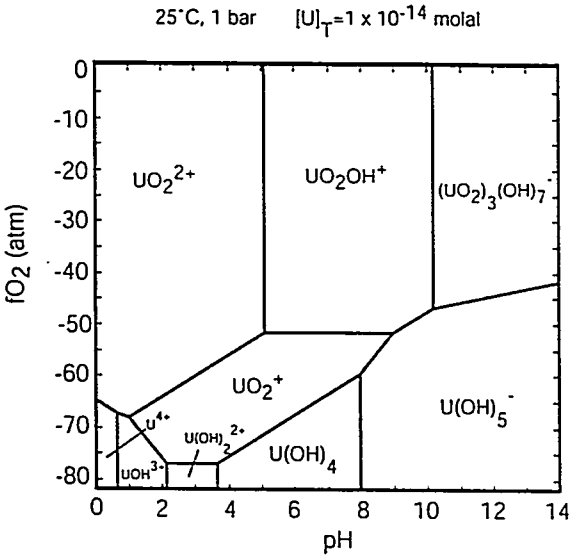

Figure 2. Uranium speciation at 25°C and 1 bar as a function of fO_2 and pH; $[U]_{total} = 10^{-14}$ molal. Uranium speciation data as in figure 1.

2.1 Ore Formation and Weathering

Subsurface accumulations of uranium (ore bodies) tend to occur at redox fronts where oxidizing U-rich solutions encounter electron-rich solids, typically organic, that are able to reduce soluble U(VI) to insoluble U(IV)-containing minerals. An exception is insoluble uranyl vanadates that form many of the ores found in the

Table 2. Equilibrium constants (K) for selected U(VI) aqueous complexes.

Chemical Reaction	Log K (25°C and 1 bar)
$UO_2^{2+} + 2H^+ \Leftrightarrow U^{4+} + H_2O + 0.5O_{2(g)}$	-33.78[a]
$UO_2OH^+ + H^+ \Leftrightarrow UO_2^{2+} + H_2O$	5.091[a]
$UO_2(OH)_{2,aq} + 2H^+ \Leftrightarrow UO_2^{2+} + 2H_2O$	11.5[b]
$UO_2(OH)_3^- + 3H^+ \Leftrightarrow UO_2^{2+} + 3H_2O$	20.00[b]
$UO_2(OH)_4^{2-} + 4H^+ \Leftrightarrow UO_2^{2+} + 4H_2O$	33.00[b]
$(UO_2)_2OH^{3+} + H^+ \Leftrightarrow 2UO_2^{2+} + H_2O$	2.70[b]
$(UO_2)_2(OH)_2^{2+} + 2H^+ \Leftrightarrow 2UO_2^{2+} + 2H_2O$	5.68[a]
$(UO_2)_3(OH)_4^{2+} + 4H^+ \Leftrightarrow 3UO_2^{2+} + 4H_2O$	11.90[b]
$(UO_2)_3(OH)_5^{5+} + 5H^+ \Leftrightarrow 3UO_2^{2+} + 5H_2O$	15.82[a]
$(UO_2)_3(OH)_7^- + 7H^+ \Leftrightarrow 3UO_2^{2+} + 7H_2O$	28.337[a]
$(UO_2)_4(OH)_7^+ + 7H^+ \Leftrightarrow 4UO_2^{2+} + 7H_2O$	21.9[b]
$UO_{2(cr)} + 4H^+ \Leftrightarrow U^{4+} + 2H_2O$	-4.638[a]
$UO_2^+ + 3H^- \Leftrightarrow U^{4+} + 1.5H_2O + 0.25O_{2(g)}$	-15.07[a]
$U(OH)_3^+ + 3H^+ \Leftrightarrow U^{4+} + 3H_2O$	4.88[a]
$U(OH)_4 + 4H^+ \Leftrightarrow U^{4+} + 4H_2O$	8.534[a]
$U(OH)_5^- + 5H^+ \Leftrightarrow U^{4+} + 5H_2O$	16.498[a]
$U(OH)_3^+ + H^+ \Leftrightarrow U^{4+} + H_2O$	0.6494[a]
$UO_2CO_{3,aq} \Leftrightarrow UO_2^{2+} + CO_3^{2-}$	-9.67[b]
$UO_2CO_{3,aq} + H^+ \Leftrightarrow UO_2^{2+} + HCO_3^-$	0.694[a]
$UO_2(CO_3)_2^{2-} \Leftrightarrow UO_2^{2+} + 2CO_3^{2-}$	-16.94[b]
$UO_2(CO_3)_2^{2-} + 2H^+ \Leftrightarrow UO_2^{2+} + 2HCO_3^-$	3.608[a]
$UO_2(CO_3)_3^{4-} \Leftrightarrow UO_2^{2+} + 3CO_3^{2-}$	-21.60[b]
$UO_2(CO_3)_3^{4-} + 3H^+ \Leftrightarrow UO_2^{2+} + 3HCO_3^-$	9.33[a]
$(UO_2)_3(CO_3)_6^{6-} \Leftrightarrow 3UO_2^{2+} + 6CO_3^{2-}$	-54.0[b]
$(UO_2)_2CO_3(OH)_3^- + 4H^+ \Leftrightarrow 2UO_2^{2+} + HCO_3^- + 3H_2O$	11.524[a]
$(UO_2)_3CO_3(OH)_3^- + 3H^+ \Leftrightarrow 3UO_2^{2+} + CO_3^{2-} + 3H_2O$	-0.66[b]
$(UO_2)_{11}(CO_3)_6(OH)_{12}^{2-} + 12H^+ \Leftrightarrow 11UO_2^{2+} + 6CO_3^{2-} + 12H_2O$	-36.43[b]

[a] Bethke [3]; [b] Davis [4]

Colorado Plateau in the USA [5]. Uranyl vanadates form during oxidative alteration of reduced U- and V-bearing minerals. Other reported U(VI) minerals that are not as common as the vanadates are the uranyl molybdates, tungstates, sulfates, selenites, and tellurites [5]. The most common U(IV)-bearing phases are uraninite (UO_2), pitchblende (highly impure uraninite), coffinite ($USiO_4 \cdot nH_2O$), and Brannerite ($(U,Ca, Y, Ce)(Ti, Fe)_2O_6(OH)$), all of which are typically found in U ore deposits (table 3). Other common uranyl phases, such as uranophane ($Ca(UO_2)_2(SiO_3OH)_2(H_2O)_5$), while limited in association to the presence of altered nuclear fuel rods and naturally weathered uraninite, are structurally and chemically complex (table 3).

Table 3. Common U-bearing minerals in rocks [5].

Phase	Chemical Formula	Comments
	Reduced U(IV) Phases	
Uraninite	UO_{2+x}	Not purely stoichimetric in nature. It can incorporate minor REE and other cations.
Pitchblende	UO_{2+x}	Very finely grained highly impure uraninite; very common U ore phase
Coffinite	$USiO_4 \cdot nH_2O$	Zircon structure, most important ore mineral after uraninite
Brannerite	$(U,Ca, Y, Ce)(Ti, Fe)_2O_6(OH)$	Metamict; most common ore phase after uraninite and coffinite
Orthobrannerite	$(U^{6+}, U^{4+})(Ti, Fe)_2O_6(OH)$	Metamict; mixed valence U phase
Ianthinite	$U^{4+}(U^{6+}O_2)O_4(OH)_6(H_2O)_9$	Mixed valence U phase; structure similar to β-U_3O_8; it oxidizes to schoepite
	Uranyl Oxyhydroxides	
Schoepite	$(UO_2)_8O_2(OH)_{12}(H2O)_{12}$	Common uranyl phase
Metaschoepite	$(UO_2)_8O_2(OH)_{12}(H2O)_{10}$	Partially dehydrated schoepite
Becquerilite	$Ca(UO_2)_6O_4(OH)_6(H2O)_8$	It likely alters to schoepite at low pH's (Finch and Murakami, 1999)
Clarkeite	$(Na,Ca)(UO_2)(O,OH)(H2O)_n$ (n=0-1)	-
	Uranyl Carbonates	
Blatonite	$UO_2CO_3 \cdot H_2O$	Monocarbonate; not a dehydration product of joliolite
Joliolite	$UO_2CO_3 \cdot nH_2O$ (n≈2)	Monocarbonate
Rutherfordine	UO_2CO_3	Monocarbonate
Urancalcarite	$Ca_2(UO_2)_3(CO_3)(OH)_6(H_2O)_3$	Monocarbonate
Wyartite	$CaU^{5+}(CO_3)(UO_2)O(OH)_4(H_2O)_7$	Monocarbonate; first known U phase to have pentavalent U

Table 3 (cont.). Common U-bearing minerals in rocks [5]

Phase	Chemical Formula	Comments
	Uranyl Carbonates (cont.)	
Fontanite	$Ca(UO_2)_3(CO_3)_4(H_2O)_3$	Monocarbonate
Zellerite	$Ca(UO_2)_3(CO_3)_2(H_2O)_5$	Dicarbonate
Metazellerite	$Ca(UO_2)_3(CO_3)_2(H_2O)_n$ (n<5)	Dicarbonate; dehydrated zellerite
Znucallite	$CaZn_{11-12}(UO_2)_3(CO_3)_3(OH)_{20\ \&-22}(H_2O)_4$	Tricarbonate
	Uranyl Silicates	
Uranophane	$Ca(UO_2)_2(SiO_3OH)_2(H_2O)_5$	Possibly the most common U mineral after uraninite
Soddyite	$(UO_2)_2SiO_4(H_2O)_2$	-
Ursilite	$(Mg,Ca)_4(UO_2)_4(Si_2O_5)_5(OH)_6(H_2O)_{15}$	-
Uranosilite	$(UO_2)Si_7O_{15}(H_2O)_{0-1}$	Rare mineral
Sklodowskite	$Mg(UO_2)_2(Si_3OH)_2(H_2O)_6$	-
Weeksite	$K_{1-x}Na_x(UO_2)_2(Si_5O_{13})(H_2O)_4$ (x=0.4)	-
Haiweeite	$Ca(UO_2)_2[Si5O_{12}(OH)_2](H_2O)_{4.5}$	-
	Uranyl Phosphates and Arsenates (Autumite group)	
Autinite	$Ca[(UO_2)(PO_4)]_2(H_2O)_{10-12}$	-
Saleeite	$Mg[(UO_2)(PO_4)]_2(H_2O)_{10}$	-
Novacekite	$Mg[(UO_2)(AsO_4)]_2(H_2O)_8$	-
Vochtenite	$(Fe^{2+},Mg)Fe^{3+}[(UO_2)(PO_4)]_4(OH)(H_2O)_{12-13}$	-

Table 3 (cont.). Common U-bearing minerals in rocks [5].

Phase	Chemical Formula	Comments
	Uranyl Vanadates	
Carnotite	$K_2(UO_2)_2(V_2O_8)(H_2O)_3$	Carnotite group mineral
Tyuyamunite	$Ca(UO_2)_2(V_2O_8)(H_2O)_8$	Carnotite group mineral
Metatyuyamunite	$Ca(UO_2)_2(V_2O_8)(H_2O)_8$	Carnotite group mineral
Uvanite	$(UO_2)_2V_6O_{17}\cdot 15H_2O$	-
	Uranyl Molybdates	
Calcurmolite	$Ca(UO_2)_3(MoO_4)_3(OH)_2(H_2O)_{11}$	-
Cousinite	$Mg(UO_2)_2(MoO_4)_2(OH)_2(H_2O)_5$	-
Iriginite	$(UO_2)Mo_2O_7(H_2O)_3$	-
Tengchongite	$Ca(UO_2)_6(MoO_4)_2O_5(H_2O)_{12}$	-
Umohoite	$(UO_2)MoO_4(H_2O)_4$	-
	Uranyl Sulfates, Selenites, and Tellurites	
Deliensite	$Fe(UO_2)_2(SO_4)_2(OH)_2(H_2O)_3$	-
Rabejacite	$Ca(UO_2)_4(SO_4)_2(OH)_6(H_2O)_6$	-
Uranopilite	$(UO_2)_6(SO_4)(OH)_{10}(H_2O)_{12}$	-
Zippeite	$K_4(UO_2)_6(SO_4)_3(OH)_{10}(H_2O)_4$	-
Haynesite	$(UO_2)_3(OH)_2(SeO_3)_3(H_2O)_5$	-
Cliffordite	UTe_3O_9	-
Schmitterite	$(UO_2)TeO_3$	-

Oxidative transformation of uraninite and oxidation/corrosion of synthetic UO_2 (spent nuclear fuel) are similar processes. Differences in solubilities between synthetic and natural UO_2 are observed though, and are believed to be caused by carbonate impurities in the natural samples[6]. Exposure to water versus dry air also affects UO_2 oxidation rates [7]. Typically the slow rate of oxygen diffusion at low temperatures makes the process rather sluggish [5]. Consequently, many studies are performed at relatively high temperatures (T > 150°C) [7]. In general, uranyl mineral formation is preceded by the appearance of intermediate U oxides such as U_3O_7 and U_3O_8 irrespective of temperature, even though the latter minerals have yet to be observed in nature[5].

2.2 Microbes and U

Microorganisms can affect the transport and deposition of uranium by, respectively, producing dissolved compounds, e.g., organic acids, capable of chelating uranium[8], or by reducing uranyl to less soluble U(IV) minerals [9]. Also, U can sorb onto bacterial cell walls and migrate. Uranyl-chelates that are anionic, e.g. uranyl-citrate, tend to sorb to soil surfaces less than bare uranyl, and are therefore favored to be transported further. Microbial breakdown of uranyl chelates often determines maximum transport distance of microbially mobilized U and for this reason remains an important area of research [8; 10]. Microbial reduction of U has been demonstrated using groundwater from the Tuba City, AZ (U.S.A) U mill tailing site [11]. Column experiments with groundwater and sand sampled at this site showed a dramatic lowering of U(VI) concentration from 250 to 14 μg/L in a period of 21 days at 24°C and 0.5 μg/L after 2 months in the presence of indigenous microorganisms [11-13]. In these experiments, microorganisms were activated by addition of ethanol and metaphosphate to the groundwater/sand mixture.

2.3 Adsorption

After precipitation, adsorption is the most important sink for U in natural systems [4; 14-17]. A large number of studies have applied surface complexation models to explain U(VI) sorption on mineral surfaces. Tripathi [18] and Hsi and Langmuir [19] studied U uptake on iron oxides. Redden et al. [20] studied U(VI) adsorption on goethite, gibbsite, and kaolinite in the presence and absence of citric acid. Redden et al. [20], Payne et al. [21], Payne and Waite [16], and Payne and Waite [17] studied U(VI) sorption onto kaolinite and ferrihydrite, and Pabalan et al. [15] studied U(VI) sorption onto α–alumina (aluminum oxide), Na-clinoptilolite, and quartz. Davis [4] combined surface complexation modeling and structural characterization of U(VI) on a variety of minerals. Jenne [22], and more recently, Krupka et al. [23], examined U(VI) adsorption Kd's obtained from sediment samples and those from various mineral adsorption studies reported in the literature. All these studies demonstrate that the peak for U(VI) uptake is at the near-neutral pH range of ~ 6 - 7.5 [24]. The sorption peak for phosphates is much lower - pH 2.5 to 4 [25]. Valsami-Jones et al. [26] and Arey et al. [27] showed that hydroxyapatite can sequester U inside its mineral structure.

In general, U(VI) sorption proceeds in the sequence: montmorillonite (clay) ≈ kaolinite (clay) ≈ gibbsite ≈ goethite > clinoptilolite > α–alumina > quartz > phosphates [15; 22; 25]. Relative sorption of U tends to depend on the type of aqueous complexes it forms in solution [4; 15; 18; 19]. At high pH's, where anionic uranyl-carbonate complexes predominate, U is only weakly sorbed due to electrostatic repulsion by negatively charged mineral surfaces [e.g. 4; 12]. Uranyl-hydroxy complexes predominate in the pH range between 6-8 along with the mixed uranyl hydroxy carbonate complex [4; 19]. When carbonate concentrations are low or absent, the predominant sorbing species are the uranyl-hydroxy complexes, .e.g., $(UO_2)_3(OH)_5^+$ [4]. Krupka et al. [23] critically reviewed the environmental chemistry of uranium and showed that U sorption is primarily controlled by pH and carbonate levels. Table 4 gives Krupka et al's. [23] maximum and minimum soil Kd values. Despite the wide variation in Kd values, the results give a reasonably clear picture of U sorption trends on soil minerals. Irreversible sorption of U typically occurs when iron and manganese oxides are present. Typically the irreversible fraction of U rarely exceeds 10% of the total [28].

2.4 Colloids

Colloidal transport of U has been investigated adjacent to both natural ore deposits and mill tailings [12; 29-32]. Colloids are not an important transport mechanism for U. Colloidal transport depends on the amount and type of colloid present, its capacity to migrate in the media, and the predominant U aqueous species in the soil solution. The predominance of negatively charged uranyl-carbonate species often prevents adsorption onto negatively charged particulate material. Mielekey et al. [29] analyzed particulate material in waters at Poços de Caldas mine and observed that even when relatively large amounts of U and Th were associated with colloids, net transport was minor due to low colloidal concentrations in the waters flowing through the aquifer. A similar situation is observed at the Cigar Lake ore deposit in Canada where relatively low concentrations of colloids limit U migration even when the U concentrations in the particulate phase and waters are similar [30].

Table 4. Minimum and maximum soil U Kd's [23]

Kd (ml/g)	pH							
	3	4	5	6	7	8	9	10
Minimum	<1	0.4	25	100	63	0.4	<1	<1
Maximum	32	5000	160,000	1,000,000	630,000	250,000	7,900	5

3.0 Uranium Plumes

U-contaminated sites can be separated into three groups:

1. Uranium Mill Tailings Remedial Action (UMTRA) sites in the USA - sites where U ore was processed.

2. Refined U releases - sites where U was released during explosive testing or nuclear waste storage activities.

3. Natural analogues - natural uranium ore deposits.

3.1 Artificial Plumes

The UMTRA sites served as U ore processing and milling plants and typically witnessed the use of acid/alkaline leaching, sand-slime separation, and ion-exchange recovery processes (lime, sulfuric acid, nitric acid, sodium carbonate, kerosene, and ammonia gas were often used as part of the leaching processes). The UMTRA sites are classified in two types: Title I and Title II. Title I sites are those in which remedial action such as removal and relocation of the mill tailing piles has been performed. Conversely, Title II sites still have their mill tailings in place and remedial action or further mining and processing remain in consideration. There are 24 Title I UMTRA sites located mostly in the western United States (Fig. 3). Most were established in the 1950's and comprise the bulk of the U-plume data obtained as many of them have been the subject of recent (~15 years) monitoring and remediation. In general, these sites contained (Title I) or still containing (Title II) piles of mill tailings and other contaminated material forming alluvium-like surface deposits where the bulk of the material has been removed and relocated elsewhere in specially engineered repositories. Title II UMTRA sites still have their mill tailings in place which typically contribute high levels of U to aquifers near the tailing source. This appears to result in longer plumes. The Title II sites will be discussed briefly because temporal monitoring of groundwater chemistry is scarce and evaluation of existing literature data is still in progress. Natural recharge through tailings piles is (or was) the primary source of dissolved U. Most of the aquifers beneath mill piles are contaminated, exceeding MCL levels of U (MCL = Maximum Concentration Limit defined by the U.S. Environmental Protection Agency = 44 ppb for U) [33]. Additional contaminants in the effluent include lead, cadmium, molybdenum, nitrate, ammonium, and selenium. Some nearby rivers to Title I UMTRA sites are contaminated with U, but not at dangerous levels. For the majority of UMTRA sites, deep aquifers (even those close to the processing plants) do not show high levels of contamination.

Groundwater chemistry can be highly variable from site to site. Some sites, such as Riverton, Wyoming [34; 35] and Monument Valley, Arizona [36] primarily contain uranyl carbonate (uranyl bi- and tri-carbonate) species whereas others, such as Falls City, Texas, are relatively poor in CO_2, have lower pH's (pH 2-5), and have predominantly uranyl-hydroxyl complexes. Nevertheless, except for the anomalously low pH site of Falls City (Texas), the groundwater chemistry between sites is quite similar as will be exemplified later in the text. White et al. [34] envisioned three general transport mechanisms for U, which may well apply to all UMTRA sites:

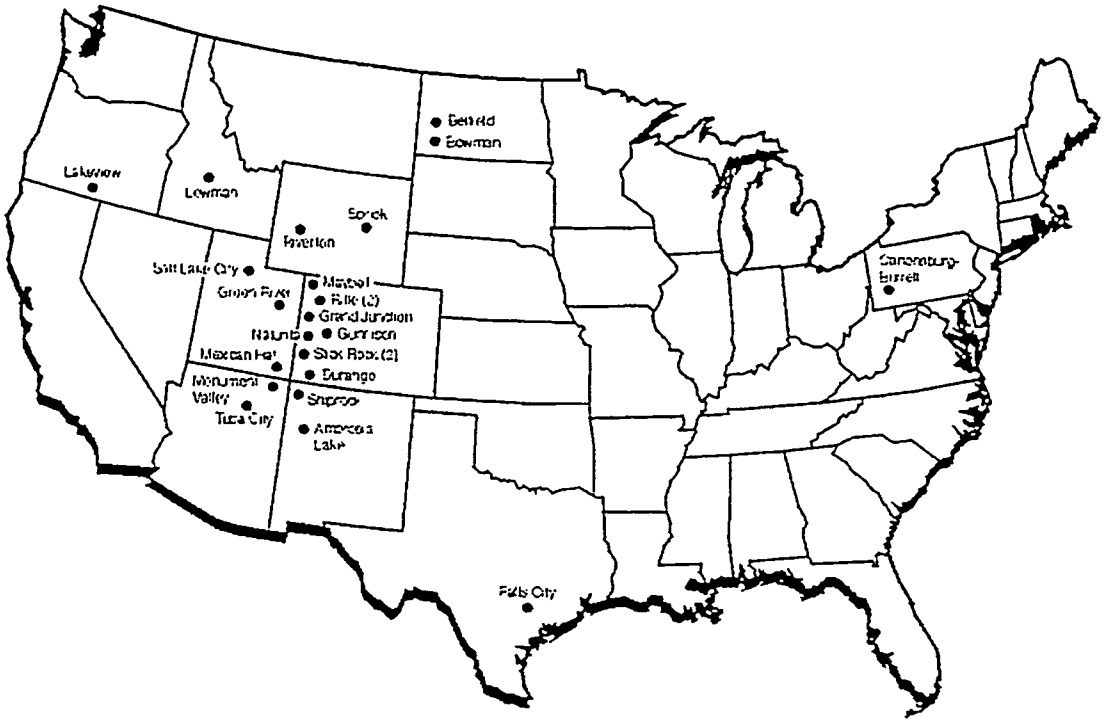

Figure 3. UMTRA Ground Water Project Title I site locations [37].

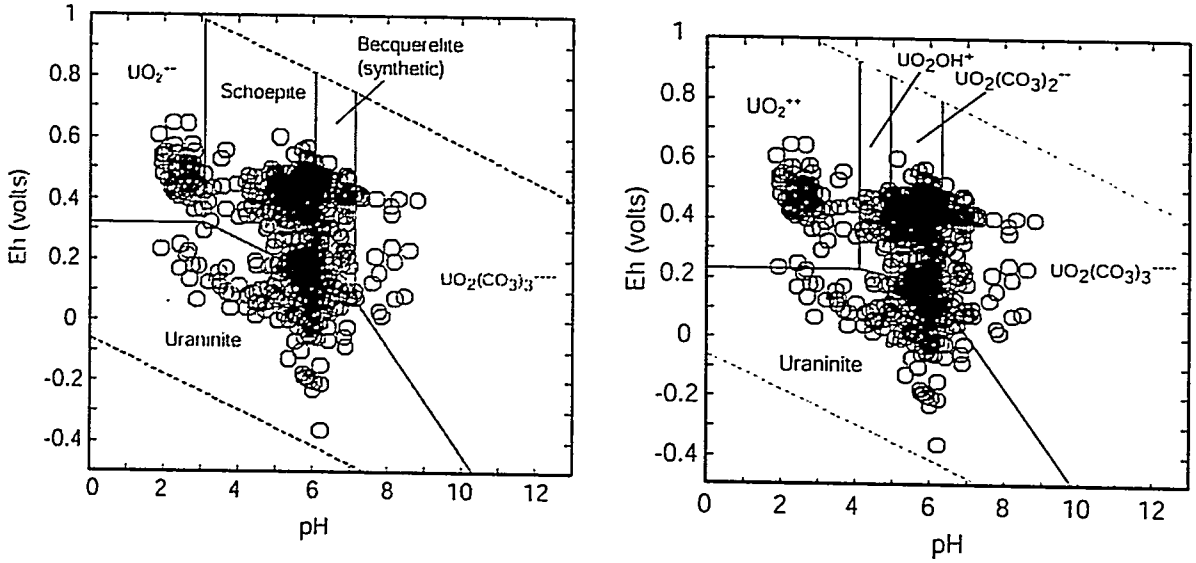

Figure 4a and b. Eh-pH diagram at 25°C and 1 bar showing U phase boundaries and data from nine title I UMTRA sites (n = 778 data points; see text): (a) $[U]_{total} = 10^{-7}$ molal, $[Ca^{++}] = 10^{-1.8}$ molal, and $fCO_2 = 10^{-2.5}$ atm. Schoepite starts appearing at $[U] = 10^{-6.5}$ molal.; (b)). $[U]_{total} = 10^{-3}$ molal, $[Ca^{++}] = 10^{-2}$ molal, and $fCO_2 = 10^{-2.5}$ atm. Uranium speciation data as in figure 1. Becquerelite (synthetic) solubility data is from Vochten and Van Haverbeke [38]

(1) initial dewatering of the slurry material in the tailings pile and concomitant downward flow soon following deposition, (2) mixing and dilution of the tailing pore waters with local ground and seepage waters, and (3) periodic meteoric water recharge into the tailing pile by precipitation or snowmelt. Subsequent U transport through the alluvium will be highly dependent upon solution chemistry (i.e., pH, ionic strength, and composition) and redox state of the system.

Bulk groundwater Eh, U, and pH analyses from nine Title I UMTRA sites taken over a 3-8 year time span are shown in figures 3 and 4. Note first of all that the data extends into the uranyl (UO_2^{++}), uranyl hydroxide (UO_2OH^+), and uranyl-carbonate $UO_2(CO_3)_2^{2-}$ species fields when [U] = 10^{-7} m and [Ca^{++}] ~10^{-2} m (Fig. 4a). If [U] =10^{-3} m and with the same Ca concentration (Fig. 4b), all of the data falls between the stability fields of uraninite (UO_2), schoepite, becquerelite, and uranyl fields. If the most scattered data represented by the Falls City (Texas) site is removed, the other 8 sites show a cluster of data points forming a characteristic vertical trend plotting at a pH ~ 7 (Fig. 5). The Falls City, Texas data set differs from the others by possessing a bimodal pH distribution (Fig. 6) and a pH-independent [U] level opposite to the other UMTRA sites. Bimodal pH distributions are not uncommon in contaminated groundwater aquifers associated with mill tailings or mining sites that have been widely exposed to pervasive *in-situ* leaching (ISL). Examples of these are Tuba City (Arizona), Konigstein (Saxony, Germany), and Split Rock (Wyoming - Title II). At all these sites, the low pH groundwater are spatially associated with the mill tailing repository area and/or chemically associated with

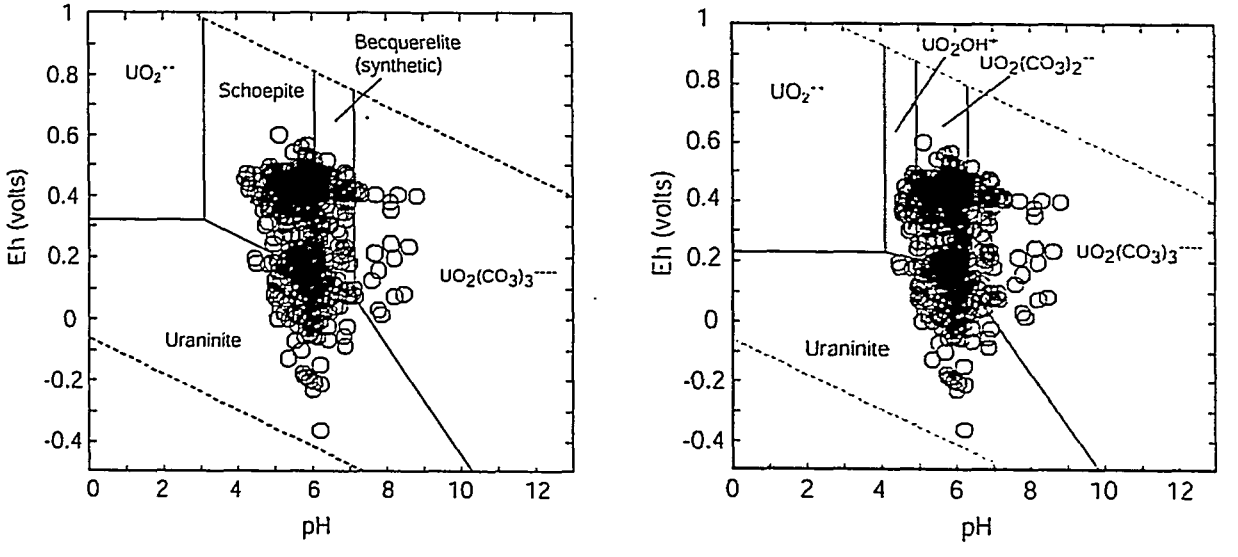

Figure 5a and b. Eh-pH diagram at 25°C and 1 bar showing U phase boundaries and data from eight title I UMTRA sites Falls City (Texas) data removed; n = 634 data points): (a) $[U]_{total} = 10^{-3}$ molal, $[Ca^{++}] = 10^{-1.8}$ molal, and $fCO_2 = 10^{-2.5}$ atm. Notice in this figure that solid uranyl phases appear in the diagram for this $[U]_{total}$.; (b) $[U]_{total} = 10^{-7}$ molal, $[Ca^{++}] = 10^{-1.8}$ molal, and $fCO_2 = 10^{-2.5}$ atm. Notice in this figure that only uranyl aqueous species are depicted in the diagram. Schoepite starts appearing at [U] = $10^{-6.5}$ molal. The uranyl species field covered by the data points is $UO_2(CO_3)_2^{2-}$. Uranium speciation data as in figure 1. Becquerelite (synthetic) solubility data as in figure 3a.

residual mine leaching waters. Even though the low pH waters in Falls City (Texas) and the above mentioned sites usually contain significant amounts of SO_4^- and PO_4^-, U does not exceed the maximum range of concentrations of ~10^{-4} – 10^{-5} m common to all the studied mill tailing sites. Therefore, the low pH seen in these anomalous groundwater may reflect the presence of residual sulfate remaining in the aquifer pores as precipitates or as fluid pockets which were dispersed by present water recharges or remediation activities.

The vertical trend in Fig. 5 originates from the uraninite stability field overlapping in a parallel fashion to the schoepite-becquerelite equilibrium boundary (Fig. 5a) or plotting inside the field of the U-carbonate complex (Fig. 5b) using a total CO_2 fugacity (fCO_2) of $10^{-2.5}$ atm typical of soils. If a lower CO_2 fugacity of $10^{-3.5}$ atm typical of equilibrium with the atmosphere is considered, the becquerilite-$UO_2(CO_3)_3^{4-}$ equilibrium boundary in Fig. 5a shifts to a lower pH diminishing the becquerelite stability field. High levels of dissolved organic carbon in UMTRA groundwater (~200 ppm) suggest that a relatively high fCO_2 value of $10^{-2.5}$ atm is a reasonable input to use in the chemographic analyses below. The becquerelite solubility value at 25°C and 1 bar chosen for this analysis is taken from Vochten and Van Haverbeke [38] for a synthetic material. Casas et al. [39] and Sandino and Grambow [40] reported becquerelite solubility values for a natural sample from the Shinkolobwe U deposit in

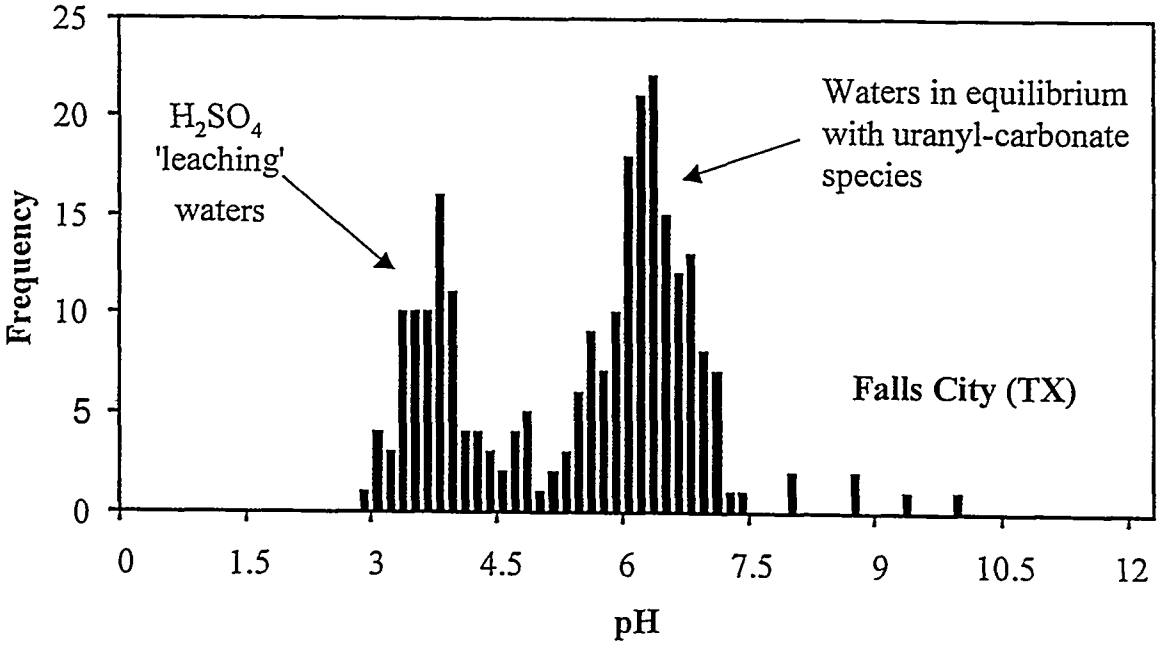

Figure 6. Bimodal distribution of pH for groundwater measured at Falls City (Texas) Title I UMTRA site (n = 249 data points). The Falls City site was exposed to *in situ* leaching (ISL) and bimodal pH has been observed in groundwater associated to other U mining (e.g., Konigstein mine, Germany) sites where ISL has been used for solution mining.

Zaire (Africa) and from the equilibria during the transformation of synthetic schoepite to becquerelite, respectively. The lower solubility value obtained by Casas et al. [39] for natural becquerelite predicts supersaturation of the mineral with the groundwater chemistry at the considered UMTRA sites. However, the much larger solubility values obtained for synthetic becquerelite [38; 40] are somewhat similar and show a near equilibrium relationship between schoepite-becquerelite for the average Ca concentrations observed in these groundwaters. This is a more realistic association considering the commonly observed presence of schoepite as a hydration product of U oxide in natural and synthetic systems. The reason for the gross oversaturation, with respect to natural becquerelite, is that Casas et al. [39] obtained a solubility value for natural becquerelite that is considerably lower than those obtained for synthetic analogues, possibly a result of lower surface areas present in macroscopic crystals yielding much lower solubilities.

Figures 7a and 7b show U mineral solubilities as a function of pH and was constructed using a mean value of 0.0151 m for the maximum Ca concentrations obtained from several groundwater analyses at various UMTRA sites. Using a median value of 0.0065 m for all Ca concentrations at the UMTRA sites that were considered, causes a negligible enlargement of the schoepite field in Fig. 6. These figures show that for the assumed fCO_2 value of $10^{-2.5}$ atm the majority of data points fall within the stability field of the $UO_2(CO_3)_2^{2-}$ species. Using a lower

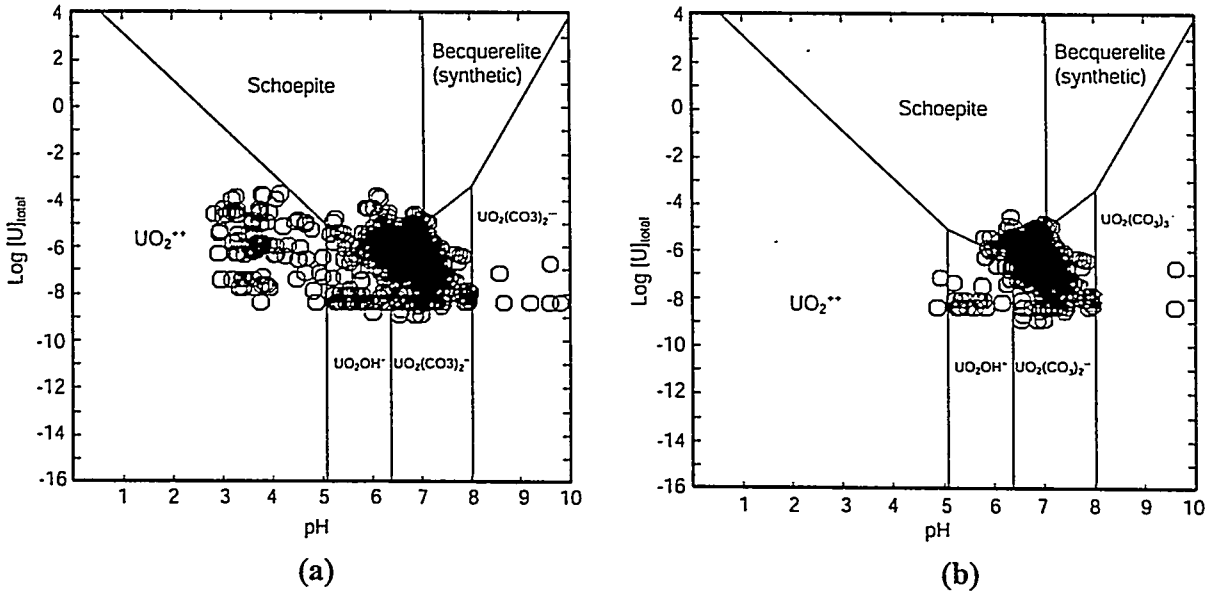

Figure 7a and b. Uranyl phase solubilities as a function of pH at 25°C and 1 bar: (a) $[Ca^{++}] = 10^{-1.8}$ molal and $fCO_2 = 10^{-2.5}$ atm (all data from the Title I UMTRA sites; n = 778 data points); (b) $[Ca^{++}] = 10^{-1.8}$ molal and $fCO_2 = 10^{-2.5}$ atm (no Falls City (Texas) data); n = 634 data points). Uranium speciation data as in figure 1. Becquerelite (synthetic) solubility as in figure 3. Notice the absence of data below $[U]_{total} \approx 10^{-8}$ which denotes the lower level of analytical detection.

fCO_2 value of $10^{-3.5}$ atm would extend the schoepite field to lower uranyl concentration values causing some of the data points to fall well inside this field. In general, the maximum uranyl concentrations correspond to the schoepite-$UO_2(CO_3)_2^{2-}$ equilibrium suggesting a solubility and, therefore, transport control on dissolved uranyl in the most contaminated aquifers that are adjacent to the former mill tailing impoundments. The close association of schoepite and becquerelite during the alteration of uranium oxide has been previously reported in the literature [38; 40-44]. Becquerelite is considered to be a thermodynamically stable product of schoepite (or meta-schoepite) alteration in the presence of alkaline elements such as Ca [44; 45]. Both phases have been observed to coexist in shallow weathered zones of natural uraninite deposits, and in short- and long-term UO_2 corrosion experiments simulating alteration of anthropogenic uranium solids like nuclear spent fuel [5; 40; 43-45]. However, their existence in groundwater reservoirs directly associated with mill tailing sites still needs to be confirmed. In the lack of unambiguous evidence for noticeable weathering mineralization in the studied mill tailing sites (Title I and II UMTRA sites in this case), we propose that the uranyl-hydroxy and uranyl-carbonate complexes such as $UO_2(CO_3)_2^{2-}$ and $UO_2(OH)^+$, respectively, along with their intrinsic local carbonate inputs near and far from the tailings impoundment, would be the most likely aqueous species to buffer the groundwater chemistry to neutral pH's. Maximum U concentrations observed at various contaminated aquifers in UMTRA sites might be controlled by the schoepite-uranyl-carbonate (possibly in combination with becquerelite) equilibrium at near neutral pH's. This observation is also applicable to Title II UMTRA sites where the mill tailings are still in place and some milling operations along with possible mining activities also remain active. Dilution and sorption are the most likely mechanisms responsible for lowering U concentrations away from the plume source.

The reaction mechanisms described before, based on the large DOE Grand Junction (CO) Project Office groundwater chemical database (Title I UMTRA sites), plus recent DOE and the Nuclear Regulatory Commission (NRC) public reports (Title II UMTRA sites), clearly suggest a reaction path controlled by uraninite dissolution and movement of groundwater compositions towards the schoepite (or meta-schoepite)/fluid equilibrium at a pH between ~6.5 and ~7.5. As shown in Fig. 5a, the path begins with oxidative dissolution of uraninite to uranyl-carbonate (reaction 1) and ends with the equilibrium between schoepite and $UO_2(CO_3)_2^{2-}$ carbonate species (reaction 2). Equilibrium between schoepite and becquerelite may occur in the presence of Ca (reaction 3).

(1) $UO_{2(s)} + 1/2\ O_2 + 2\ HCO_3^- \Rightarrow UO_2(CO_3)_2^{2-} + H_2O$

(2) $8\ UO_2(CO_3)_2^{2-} + 20\ H_2O + 3\ O_2 \Leftrightarrow (UO_2)_8O_2(OH)_{12}\bullet 12H_2O + 16\ HCO_3^-$

(3) $(UO_2)_8O_2(OH)_{12}\bullet 12H_2O + 2\ H^+ + Ca^{++} \Leftrightarrow Ca(UO_2)_6O_4(OH)_6\bullet 8H_2O + 2\ UO_2^{++} + 8\ H_2O$

The second type of U plumes arise from releases of refined U, such as those involving explosive activity or nuclear waste storage. One located at Lawrence Livermore National Laboratory (LLNL) involved explosive activity in pits and is still under investigation. Preliminary U

well data for this site obtained near the explosive pits show plumes lengths of ~0.5 kilometer measured to the 11 pCi/L (≈16 ppb) contour. Some important nuclear waste sites that are under current investigation include the Hanford Tank Farm [46] in Washington and the Savannah River Site (SRS) in Georgia, but were not considered in the present study for several reasons: (1) reports on groundwater chemistry needed to assess plume length are not yet available (SRS) or are in the process of being updated or published (Hanford), and (2) the monitoring well network distribution in some cases (e.g., tank farm at Hanford) is not adequate for the purpose of this study. At this moment, the SRS study has not reported U plumes beyond the tank farm and most of the currently available data is for Tritium and TCE plumes [47]. Even when there are insufficient monitoring wells at a distance from the Hanford tanks to accurately estimate further plume extensions beyond the source, we report only one relatively large U plume in one process trench (see table 5).

3.2 Natural Plumes

Natural uranium ore deposits are often used as analogues for long-term high level nuclear waste repositories but are also useful analogues for existing contaminant plumes. The principal U ore source mineral in these deposits is reduced U oxide (UO_2) which is subsequently altered during fluid-mineral interaction under oxidizing conditions to uranyl- oxides, phosphates, and silicates. Most of the U migration, away from the concentrated uranium ore, occurred after oxidation through groundwater mass transport. Subsequently, U became incorporated into surrounding rock through sorption and precipitation of weathering phases. This sequence of oxidation, transport, and deposition is expected to be a reasonably good analogue for transport of U present in man-made radioactive waste repositories, mine mill tailings, and ore processing plants. Since U-contaminated soils are chemically analogous to U ore bodies, the extent of the contaminated "halo" around the latter might also provide useful information about plume migration.

Roughly 40% of U ore bodies occur as epigenetic sedimentary deposits such as those found in the Wyoming Tertiary basins and in coastal plain systems, e.g. the South Texas Uranium province [48]). Other U occurrences are associated with alkaline volcanic and granitic igneous provinces, e.g. the Sanerliu granite-hosted U deposit in southern China [49], the Peña Blanca district rhyolite tuff in the state of Chihuahua, Mexico [50-56], the Palmottu U deposit in Finland [57; 58], the Maqarin U hydrothermal deposit in northern Jordan [59; 60], the Valles natural analogue at Valles Caldera in New Mexico [61], the Konigstein U mine in Saxony, Germany [62; 63], and the Poços de Caldas alkaline complex in the state of Minas des Gerais, Brazil e.g. [64; 65]. We focus here on those ore bodies that have been well studied and monitored for long periods of time and whose groundwater chemistry provide an objective plume length analysis. These include the Alligator Rivers region (the Koongarra ore deposit) in Australia, the natural uranium reactors/mines of Oklo in the Republic of Gabon in equatorial Africa, the Morro do Ferro and Osamu Utsumi U mines at Poços de Caldas alkaline complex in the state of Minas Gerais, Brazil, and Cigar Lake in Saskatchewan, Canada.

3.2.1 Koongarra

The Koongarra ore deposit is located in northern Australia and is part of the Alligator Rivers Uranium Field. The host rock for the Koongarra ore deposit is a quartz chlorite schist and the zone of primary mineralization is about 100 meters deep [66]. The primary mineralized region is composed of uraninite and is situated between a graphite rich region bounding the Kombolgie Sandstone and the Koongarra reverse fault [66]. According to Yanase et al. [32], the groundwater flowpath of the groundwater begins at the surface and percolates through the porous Kombolgie Sandstone and the Koongarra reverse fault that separates the sandstone from the ore body. Fluids move deeper into the primary mineralized zone through the fault, but shift away from it to a horizontal flow regime creating a weathered zone of secondary U mineralization. The close proximity of the primary mineralized region and the graphitic schist layer suggest that reducing reactions involving this strata were responsible for the precipitation of uraninite from fluids percolating through and near the fault. A very similar scenario caused the formation of uraninite in Oklo natural reactors where the mineralized region is also bounded by a fault [67; 68]. The primary ore body at Koongarra has been affected by weathering forming a secondary ore alteration zone extending the limits of the U migration [66; 69]. The presence of this weathered zone is also a good indication of groundwater flow through the ore body. Weathering processes such as precipitation and concomitant transformation of secondary minerals, e.g., chlorite → vermiculite + Fe-minerals → kaolinite + Fe-minerals, coupled with sorption by these phases, retards U transport and migration downstream from the main ore deposit. The precipitation of saléeite ($Mg(UO_2)_2(PO_4)\cdot 10H_2O$) and the irreversible sorption of U onto Fe-oxides produced by chlorite weathering likely controlled U migration and/or dispersion at Koongarra [70]. According to Murakami et al. [70], saléeite, along with metatorbernite, precipitated between apatite and sklodowskite grains at the expense of these two latter phases. These authors suggested on the basis of micro-textural observations that localized interfacial precipitation is the most plausible way of forming these phases in undersaturated fluid conditions for the Koongarra groundwater. Moreover, Sato et al. [71] reported significant U scavenging associated with Fe oxides (nodules) having concentrations many times larger than in the groundwater.

The Koongarra ore is exposed to monsoonal climate, but seasonal sampling suggests that a sharp change in water recharge has little effect on groundwater bulk chemistry. In general, the groundwater of this deposit is dilute, with total dissolved solids in the range of 200 mg/L [32]. The deeper groundwater is enriched in CO_2 indicating that U in solution, within the weathered zone, is mobilized as uranyl-carbonate complexes [32; 72]. The primary mineralized zone is traversed by the Koongarra fault which may well serve as a conduit for surface water to permeate into the deeper formations and dilute the groundwater [32; 72]. U concentrations in the groundwater wane away from the primary mineralized zone for about 200 meters until background concentrations are observed. Groundwater flow modeling [73] suggests that water moving away from the porous sandstone and the fault are primarily transmitted through a very heterogeneous fractured

media in the weathered zone, making the characterization of flow velocities at the scale of the ore very difficult. Therefore, simplistic 1-D solute transport simulations using single velocities cannot be satisfactorily applied for the description of U migration in this area.

3.2.2 Oklo

The Oklo natural reactors in The Republic of Gabon, equatorial Africa, consist of two natural reactors, Bangombe and Okelobondo, which represent an extreme case where large amounts of transuranium series elements were produced over long periods of time, after the reactor went critical ~2 billion years ago [67]. Furthermore, the tropical climate assures abundant recharge. The Oklo reactors have been extensively studied due to potential similarities to proposed long-term high-level nuclear waste repositories [67; 74]. The reactor cores are composed of uraninite surrounded by Precambrian pelitic sandstones and unmetamorphosed volcanic rocks [67]. U Mineralization of the Oklo cores occurs within a sedimentary layer of fluvial sandstones and conglomerates associated with a carbonate-rich/argillaceous matrix [67]. An interesting similarity between Oklo and Koongarra ore deposits is that both are bounded by a major fault which serves as a natural barrier, and as a conduit, limiting U migration and/or dispersion through groundwater percolation near the fault and along the weathered zone. In both cases, the fault served as a conduit for fluid recharge and as the initial point for the oxidation zone to originate. The estimated maximum axial plume length for Bangombe and Okelobondo are 0.25 and ~1.3 km, respectively. Recent reactive transport models on Bagombe and Okelobondo by Ayora et al. [68] and Salas et al. [75], respectively, suggest that local geology and mineralization in the host strata controls fluid chemistry. At Okelobondo, $Fe^{2+}/Fe(OH)_3$ and Mn-minerals control the reaction paths for two types of site groundwater [75]. At Bangombe the pore water chemistry appears to be controlled by the $Fe^{2+}/Fe(OH)_3$ equilibria [68].

3.2.3 Poços de Caldas

The Poços de Caldas ore deposit has been the subject of a number of studies that have characterized its geology, geochemistry, hydrology, and hydrochemistry in order to understand ore formation and U transport [64]. Poços de Caldas is a round-shaped Mesozoic igneous alkaline complex of ~33 km in diameter comprising suites of alkaline volcanic and intrusive rocks mainly phonolites and syenites [76]. Most of the radioactive and REE mineralization is associated with heavy hydrothermal activity and the formation of volcanic breccias that host these deposits [76; 77]. Subsequent episodes of ultramafic magmatism and lamprophyric dyke formation, followed by intense weathering, resulted in the formation of supergene zones producing redox fronts that mobilized and enriched U to lateritic levels [76]. There are two sites for U mineralization in this area: Osamu Utsumi and Morro do Ferro mines. U mineralization at Osamu Utsumi is the result of supergene weathering beneath a lateritic soil extending to an approximate depth between 80 and 140 meters [78]. Oxidized and reduced zones along the redox front are distinguished by sharp changes in color. Most of the minerals hosting the bulk of U in this mine are uraninite, pitchblende, and brannerite. Precipitation of these U-bearing minerals is associated with oxidation of pyrite and secondary precipitation of Fe oxy-hydroxides

throughout the reaction front [78]. A reactive transport model by Lichtner and Waber [79] for the Osamu Utsumi mine successfully predicts the migration of the redox front and the resulting phases precipitated along the reaction path. In this case, pyrite oxidation causes the fluid to be reduced, resulting in precipitation of uraninite in the redox front [79; 80]. Morro do Ferro is richer in Th and depleted in U relative to Osamu Utsumi [29]. Groundwater sampled close to the surface of this deposit is oxidized as expected, but more reduced in deeper samples in the boreholes. The high concentration of Th in the groundwater is thought to be associated to colloidal matter because of its low solubility and its high partition with colloidal matter at the Osamu Utsumi site [29]. The Morro do Ferro plume was measured using a vertical profile along a transect comprising a limited set of sampling boreholes. The plume length is ~ 0.15 km.

3.2.4 Cigar Lake

The Cigar Lake unconformity-type U ore deposit in northern Saskatchewan, Canada [81-83] is hydrothermal in origin, was formed ~1.3 Ma ago, and is confined to an altered sandstone ~430 meters below the surface [83; 84]. The primary U minerals are uraninite and pitchblende. Waters in contact with the ore originate from an overlying permeable sandstone aquifer. Because the Cigar Lake ore deposit is not exposed at the surface, U release is extremely slow. Weathering, formation of a surrounding clay-rich matrix, and capping by an impermeable quartz-cemented zone cause the groundwater in contact with the ore body to be highly reduced. The system has consequently been assumed to be closed with respect to U. U transport in this ore body has been modeled by Liu et al. [85] using a near-field release model assuming molecular diffusion perpendicular to the clay zone and advective groundwater flow parallel to the clay zone. Bruno et al. [86] modeled the fluid chemical evolution along different flowpaths, using a simple kinetic mass transfer calculation entailing oxidative uraninite dissolution, assuming long residence times. Indeed, Liu et al. [85] model predicts very low U concentrations as observed in the field. The confinement of U and other radionuclides in the clay zone arrest their migration, therefore producing plumes in the porous overlying sandstone that are too narrow to be detected [85].

4.0 Plume Analysis

The maximum surface extension of both artificial and natural plumes or **maximum plume axial length** is used as the index criteria to assess plume behavior. Note though that the concept of maximum plume axial length, as applied here, is by necessity operational because of the random, limited, and in most cases, subjectively biased well sampling or monitoring used by different workers at different sites. Moreover, the highly distorted morphology of groundwater plumes, the presence of daughter plumes, and the presence of background levels of U causes more uncertainty as to the real extent of the 2-D surface coverage of these plumes. To establish an objective basis of comparison, visual inspection of plume contour maps and U concentration data in sample wells were used jointly to establish the maximum plume axial lengths. Specifically, the maximum plume axial length is defined there as *the maximum distance between two points encompassing the farthest*

boundaries of the plume as constrained and/or permitted by the sampling well network in a particular site where measurable U concentrations in the range of 10-20 ppb have been obtained.

Previous workers [87] conversely, have considered the farthest distance between the source (or highest contaminant concentration) and the plume boundary. This approach is useful in intuitively assessing the limits for potential spreading of a plume within a given area if the data set is sufficiently large and reliable. For most U plumes, temporal and spatial limitations in well sampling and the generation of daughter plumes through ongoing remediation activities, or natural recharge, makes identification of the source within a waste site a very difficult task for a given well monitoring network. This could lead to underestimates of plume length that can only be overcome by a large and fairly dependable data set. Given the limited amount of useful data, the irregular spatial distribution of monitoring wells, and the scarce number of the latter at each site, we found the maximum axial length provides (in the extreme case of U mobilization) a reasonably good estimate of the 2-D contaminant surface coverage. Note there is a general lack of temporal data for periods longer than 5 years for most sites. Many of the sites possessed a very large (hundreds of meters across) and disperse source term. The width of the source term is implicitly counted in the maximum plume axial length measurement. In other words, if the actual plume advance were modeled as emanating from a point source, the calculated plume lengths would be a great deal less. In some cases, particularly for the large scale natural analogues (e.g., Poços de Caldas and Oklo), the plume lengths were estimated based on a vertical profile using a linear monitoring well transect. To illustrate the manner in which plumes were measured, figures 8 through 11 show a number of the UMTRA plumes and the labeled plume lengths.

Many of the UMTRA sites are located within 2 or 3 km of rivers. There are a few cases where groundwater plumes were truncated by discharge into rivers, e.g. Figure 9 - Riverton, Wyoming, as might be expected where rivers are fed by groundwater. In arid regions though, rivers often lose water to adjacent aquifers and many of the plumes we observed spread parallel to, or away from, nearby rivers, suggesting that measured plume lengths reflect groundwater transport.
Table 5 shows all the U plumes considered in this study along with estimated maximum axial plume lengths. The frequency distribution of maximum axial plume lengths for all sites listed in table 5 is shown in figure 12, and suggest that the maximum observed distance of migration is a little more than 2 kilometers. Note again that this distance is the maximum observed spread of the 10-20 ppb U plume contour, and that it includes both upgradient and downgradient limbs of the plume. This means, the downgradient (maximum) reach of plumes from the source is substantially less than 2 km. If we calculate plume length using contours of 44 ppb U, the MCL, most of the plumes (if not all of them) would have an axial length of approximately 0.5 km or less. An anomalous long outlier is the plume associated with the Konigstein mine [62; 63], located 25 km southeast of the city of Dresden, Germany and the UMTRA site Falls City, Texas. *In situ* leaching (ISL) was conducted in the Konigstein mine using periodic inputs of sulfuric acid (H_2SO_4) that mixed and diluted with local groundwater needing further additions of the acid to continue the leaching process [62].

Table 5. Summary of estimated maximum axial plume lengths and their site characteristics. The listed UMTRA sites are the only ones for which plume length data can be extracted.

Site	Type	Max. Axial Plume Length (km)	Min.Axial Plume Length (km)	Sampled Depth (m)	Sources	Comments
Canonsburg, PA	UMTRA (Title I)	0.3-0.37	-	2-8	88	Groundwater table can be found at shallow depths in the fill. Humid continental climate.
Crow Butte Uranium Mine Unit 1, NB	In situ leaching	0.63	0.07	-	89	Pre-operational/baseline maximum plume length measured to ~ 20 ppb. Post-operational ISL mining caused [U] to be orders of magnitude larger in monitoring groundwater wells.
Falls City, TX	UMTRA (Title I)	4.95	3.94	-	90	Plume analysis comprises tailings pile areas 1, 2, 3, 4, 5, 6, and 7. Largest UMTRA plume.
Fernald Processing Site (OH)	UMTRA (Title I)	1.3	0.61-0.78	-	91	Private well monitoring locations (1992-1996)
Grand Junction, CO	UMTRA (Title I)	2.5	0.47 - 0.6	-	92	Bulk groundwater composition is SO_4^- rich and relatively HCO_3^- poor. Close to saturation with respect to calcite.
Gunnison, CO	UMTRA (Title I)	2	0.4	50-150	93; 94	Lindgren [94] reported a plume length value of 1.5 km interpolated distance to [U]=40 ppb.
Hanford (WA) 300 Area process trench	UMTRA (Title I)	0.79	0.52	50-150	95	Plume bounded by the Columbia River
Kennecott Uranium Facility (WY)	UMTRA - Mine (Title II)	0.69	0.26	~15	96	Highly irregular plume shape. Maximum plume length measured to ~8 pCi/L
Konigstein Mine, Germany	In situ leaching	3.6-4.0	~1.5	~15-350	62; 63	In situ leaching of U with sulfuric acid (H_2SO_4). Longest plume measured.

Table 5 (cont.). Summary of estimated maximum axial plume lengths and their site characteristics.

Site	Type	Max. Axial Plume Length (km)	Min.Axial Plume Length* (km)	Sampled Depth (m)	Sources	Comments
LLNL-plume 1 pit 4-5, CA	Explosive Activity	0.43	0.08	-	97	Sampled 2nd quarter 1994; plume length measured to the [^{234}U + ^{238}U]=10 pCi/L (~30 ppb) contour.
Maybell, CO	UMTRA (Title I)	0.4	0.15	40-50	98	U/TDS* ratio indicates that soluble salts move further than U beyond the mill tailing limits.
Monticello Millsite, CO	UMTRA (Title I)	2.2-2.4	0.42	-	99	Plume length distance measured to a ^{234}U + ^{238}U concentration level of ~18 pCi/L (~54 ppb).
Monument Valley, AZ	UMTRA (Title I)	1.4	1.1	17-47	36	Plume length for the $[U]_T$>44ppb region (deep De Chelly aquifer) is ~0.7 km. Max. plume length determined for the alluvial aquifer.
Naturita, CO	UMTRA (Title I)	0.7	0.2	3-76	100	Plume length may be larger than estimated value. Groundwater sampling restricted to the shallow river alluvium.
New Rifle, CO	UMTRA (Title I)	1.6	0.6	30-95	94; 101	U/TDS ratio is similar in all sampling wells suggesting that U salts and U migrate at the same rate.
Rio Algom, Moab - Lisbon Facility, UT	UMTRA - Mine (Title II)	2.52	1.71	13-45	102	Maximum plume length measured to 10 -20 pCi/L natural U sampling well - among the largest Title II plumes
Riverton, WY	UMTRA (Title I)	1.7	1.2	7-8	34; 35; 94; 103	Lindgren [94] reported a plume length value of 0.9 km interpolated distance to the 44 ppb [U] point
Slick Rock (NC), CO	UMTRA (Title I)	0.24	0.12	20-50	104	Sampling restricted to tailings pile. Plume may be bigger than estimated. Monitoring wells at plume boundary show [U] ≈ 900-1000 ppb.

Table 5 (cont.). Summary of estimated maximum axial plume lengths and their site characteristics.

Site	Type	Max. Axial Plume Length (km)	Min.Axial Plume Length (km)	Sampled Depth (m)	Sources	Comments
Slick Rock (UC), CO	UMTRA (Title I)	0.5	0.2	20-50	104	Site is bounded by a topographic high and a river.
Sohio Western L-Bar, NM	UMTRA - Mine (Title II)	1.34	0.96	-	105	Maximum and minimum plume lengths are approximate - few wells available for measuring natural U sampling
Split Rock (WY) Northwest Valley	UMTRA (Title II)	2.63	0.75	0-30	106	Mill tailings still remain in place. Long plume length for an UMTRA site.
Split Rock, (WY) Southwest Valley	UMTRA (Title II)	2.51	0.86	0-30	106	Mill tailings still remain in place. Long plume length for an UMTRA site.
Split Rock (WY) Between Northwest and Southwest Valley	UMTRA (Title II)	2	-	0-30	106	Mill tailings still remain in place. Plume length measured between two valleys containing the mill processing plants and tailings.
Tuba City, AZ	UMTRA (Title I)	1.12	0.5	15-18	12; 37; 94	Maximum plume length measured to [U] ≈ 40 ppb [37].
Weldon Springs Site, Missouri (WSOW)	UMTRA (Title I)	0.6	-	-	107	Plume length value is very approximate. [U] well data is very heterogeneous. Multiple plumes observed. Very localized plume lengths with [U]>15 pCi/L (~45 ppb) are only reported.
Weldon Springs Site, Missouri (WSCP)	UMTRA (Title I)	1.1	-	-	107	Multiple plumes observed. Same explanation as above.

Table 5 (cont.). Summary of estimated maximum axial plume lengths and their site characteristics.

Site	Type	Max. Axial Plume Length (km)	Min.Axial Plume Length (km)	Sampled Depth (m)	Sources	Comments
Koongarra ore deposit, Alligator River Uranium Field, Australia	Natural Analogue	0.48-0.5	0.38	13-25	32; 66; 72	Presence of a weathered zoned. Uranyl-carbonate complexes predominant due to high HCO_3^- concentration in deeper groundwater.
Bangombe, Oklo natural reactors, Gabon	Natural Analogue	0.25	-	25-500	67; 68; 74; 108; 109	Presence of a weathered zone. Groundwater chemistry controlled by the $Fe^{2+}/Fe(OH)_3$ equilibria. Fluids are not enriched in CO_2.
Okelobondo, Oklo natural reactors, Gabon	Natural Analogue	0.9-1.0	-	6-100	67; 68; 74; 75; 108; 109	Presence of a weathered zone. Groundwater chemistry controlled by the $Fe^{2+}/Fe(OH)_3$ (reduced) and $Mn^{2+}/MnOOH$ (oxidized) equilibria. The latter is richer in CO_2.
Osama Utsumi, Poços de Caldas, Brazil	Natural Analogue	0.5-0.6	-	0-125	77; 110-112	Presence of a weathered zone. Pyrite oxidation induces reduction of fluids and subsequent UO_2 precipitation in the redox front.
Morro do Ferro, Poços de Caldas, Brazil	Natural Analogue	0.15	-	0-85	77; 110; 111; 113	Presence of a weathered zone. Th rich deposit. The presence in groundwater is probably associated to colloids. Ore zone is very close to the surface.
Cigar Lake ore deposit, Canada	Natural Analogue	0.4	-	0-500	83; 86	Deep (~430 m) and concealed unconformity type U deposit. Capped by an impermeable quartz barrier. Considered a closed system.

* Minimum axial lengths are measured perpendicular to maximum axial length.

Leached contaminants have therefore been spread further than they would have otherwise. ISL has been used in many U mines in the United States, e.g., Falls City, Texas, and worldwide [114] and is being currently considered as a cheaper option for future U mining by various countries [115; 116]. Falls City (Texas) mill site show the largest observed plume for a Title I UMTRA site. It also has a fairly recent history of secondary solution mining operations between 1978 to 1982 which may be attributed to its spatial extent of contamination[117]. Some examples of previous and presently planned use of ISL solution mining are Germany (Konigstein), Czech Republic (Stráz mine in north Bohemia), Bulgaria, Ukraine, Russia, Kazakhstan, Uzbekistan, China, United States, and Australia [115; 116; 118]. The Konigstein mine is probably the best studied example of intensive use of ISL in U mining and its consequences on aquifer and groundwater contamination [114]. A recent example of ISL solution mining by injection of an oxidant and a carbonate-rich solution in the USA is the Crow Butte U mine unit 1 in Nebraska [89]. The groundwater chemical patterns of post-operational ISL activities show a plausible maximum plume length increase that may exceed ~3-4 times that of pre-operational/baseline standards (baseline max. plume length ≈ 0.62 km). Even the subsequent restoration/stabilization activity of groundwater quality shows U concentrations that exceed MCL limits further beyond the monitoring well network.

5.0 Discussion and Conclusions

The hydrologic conductivities, Kds, and original contaminant source masses for the various sites probably vary by orders of magnitude (see e.g. table 4). Nevertheless, actual plume trajectories seem to cluster, and suggest that the combined effects of dispersion and chemical reaction are sufficient to arrest most uranium plumes before they move more than roughly a kilometer from their source. The natural life cycle of a uranium plume appears to involve an initial movement away from a source region that takes place within a few years and does not exceed 2 kilometers, followed by a geologically long period of immobile quiescence. Natural plumes from ores that have been weathered and subjected to periodic meteoric inputs for long periods of time do not migrate appreciably beyond their known natural barriers, even during mining. Similarly, the UMTRA sites do not show a significant dispersion of contaminants beyond the limits of the contaminated area, even though these are not as deeply buried and are in more porous strata than those found in the natural analogues and ore U mining sites. The plume length and the U concentration in monitoring wells remain relatively constant, or change insignificantly, for periods of time approaching 15 years in many cases [94]. It appears that sorption, dilution, and precipitation are sufficiently effective sinks to limit short-term (years to decades) the advance of artificial U plumes. In long-term situations (thousands to millions of years), weathering processes and secondary precipitation of oxidized uranyl phases appears to limit advance of natural plumes. This picture of U plume behavior has a number of implications for activities

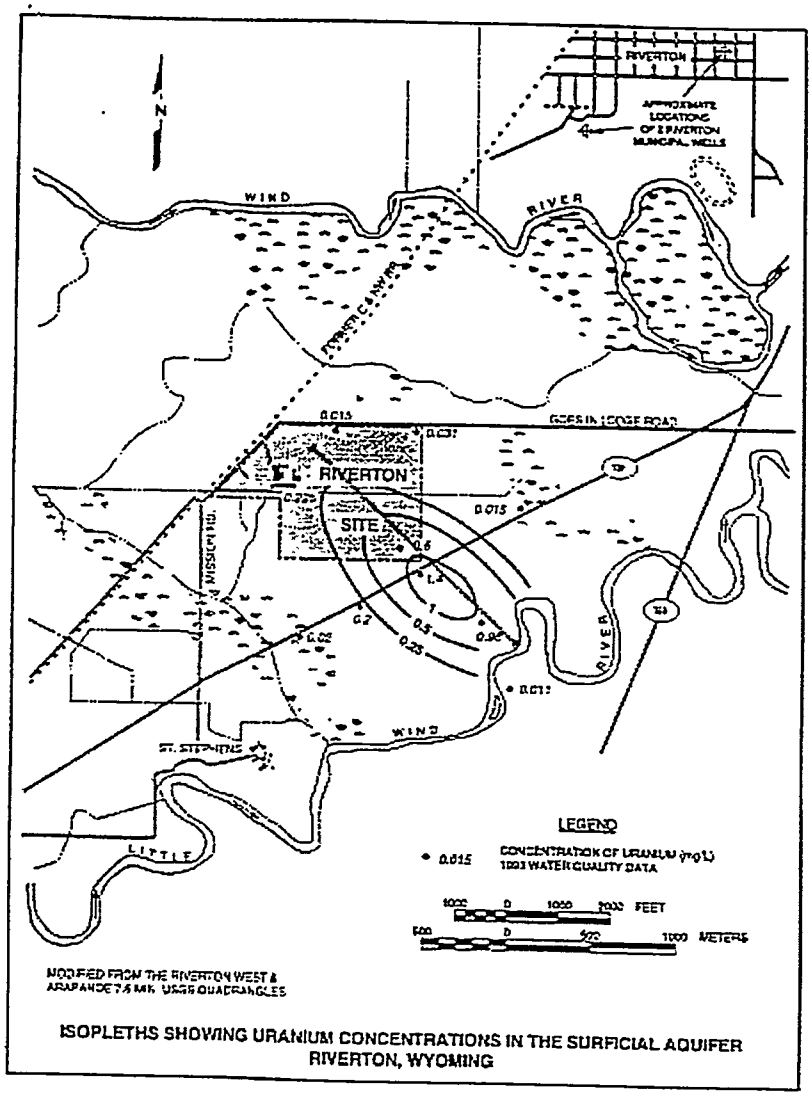

Figure 8. Riverton (Wyoming) plume [35]. The thick light-gray line parallel to the elongated U plume contours denotes the estimated maximum axial plume length (see text).

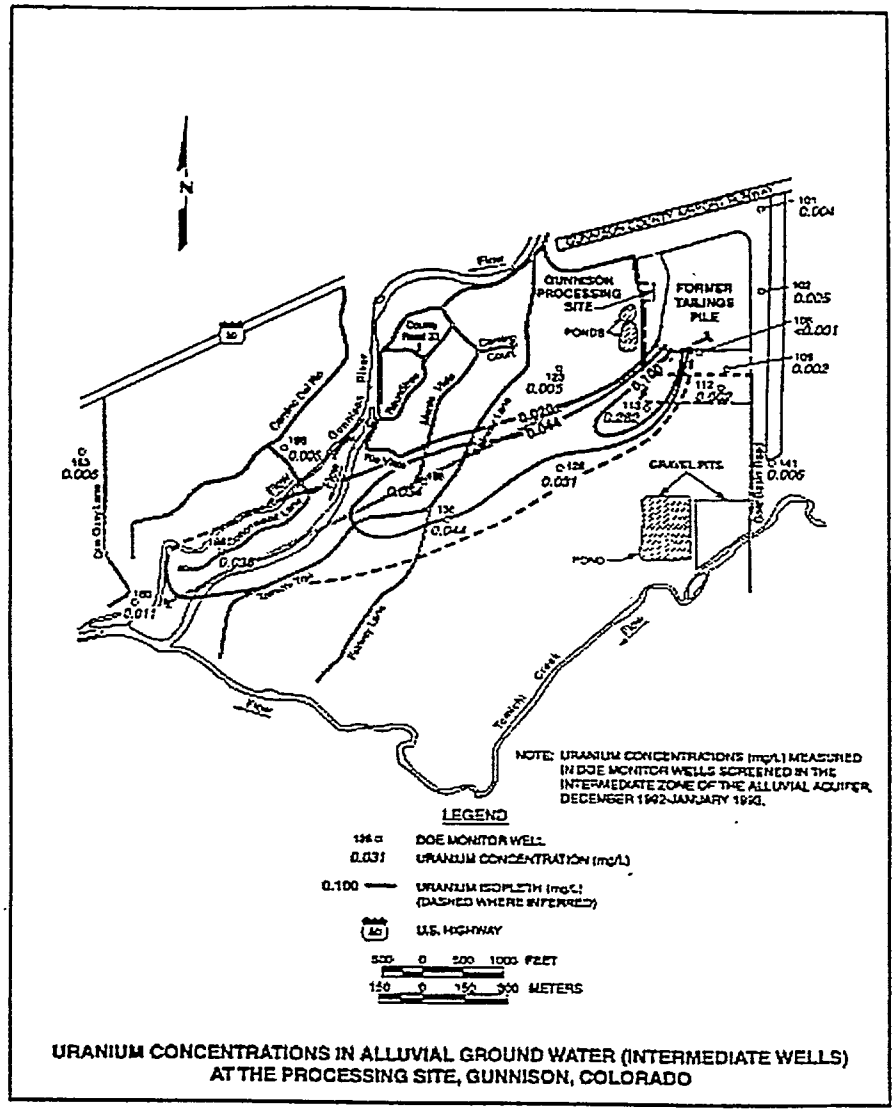

URANIUM CONCENTRATIONS IN ALLUVIAL GROUND WATER (INTERMEDIATE WELLS) AT THE PROCESSING SITE, GUNNISON, COLORADO

Figure 9. Gunnison (Colorado) plume [93]. The thick light-gray line is the estimated maximum axial plume length as in figure (see figure 8).

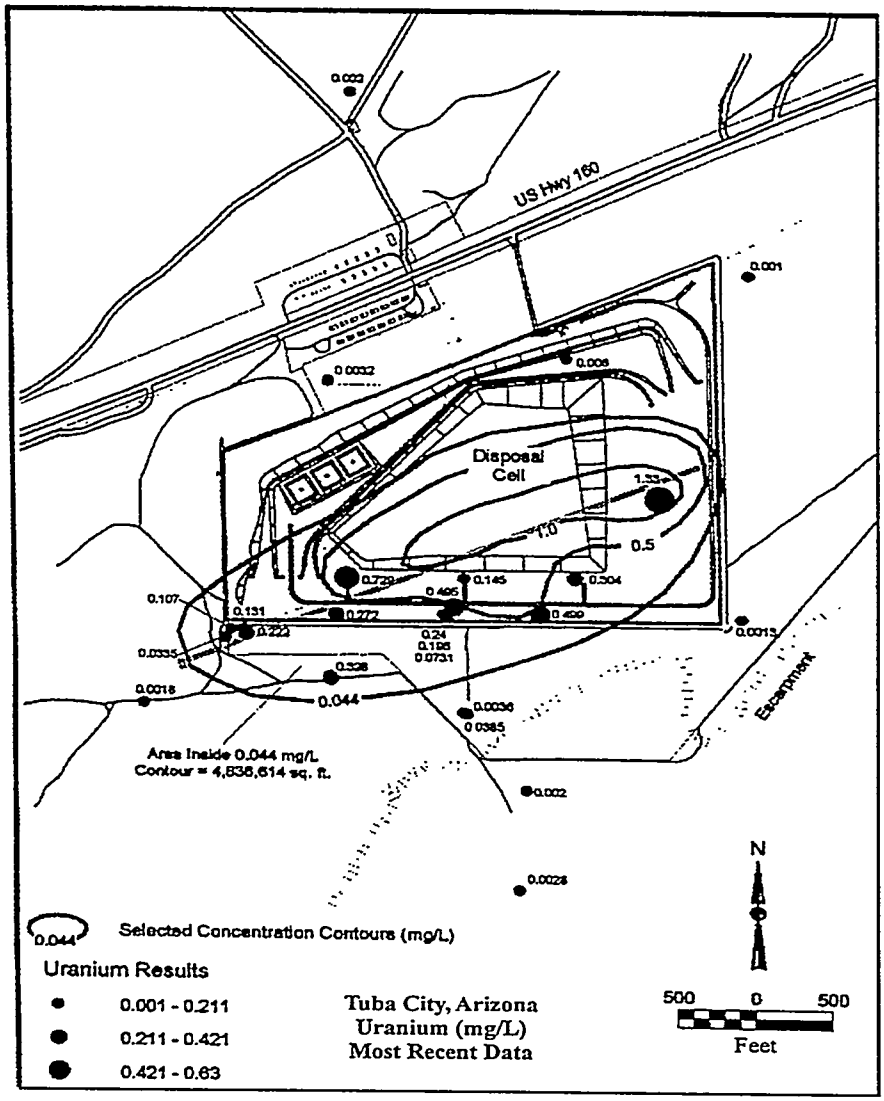

Figure 10. Tuba City (Arizona) plume [37]. The thick light-gray line is the estimated maximum axial plume length as in figure (see figure 8).

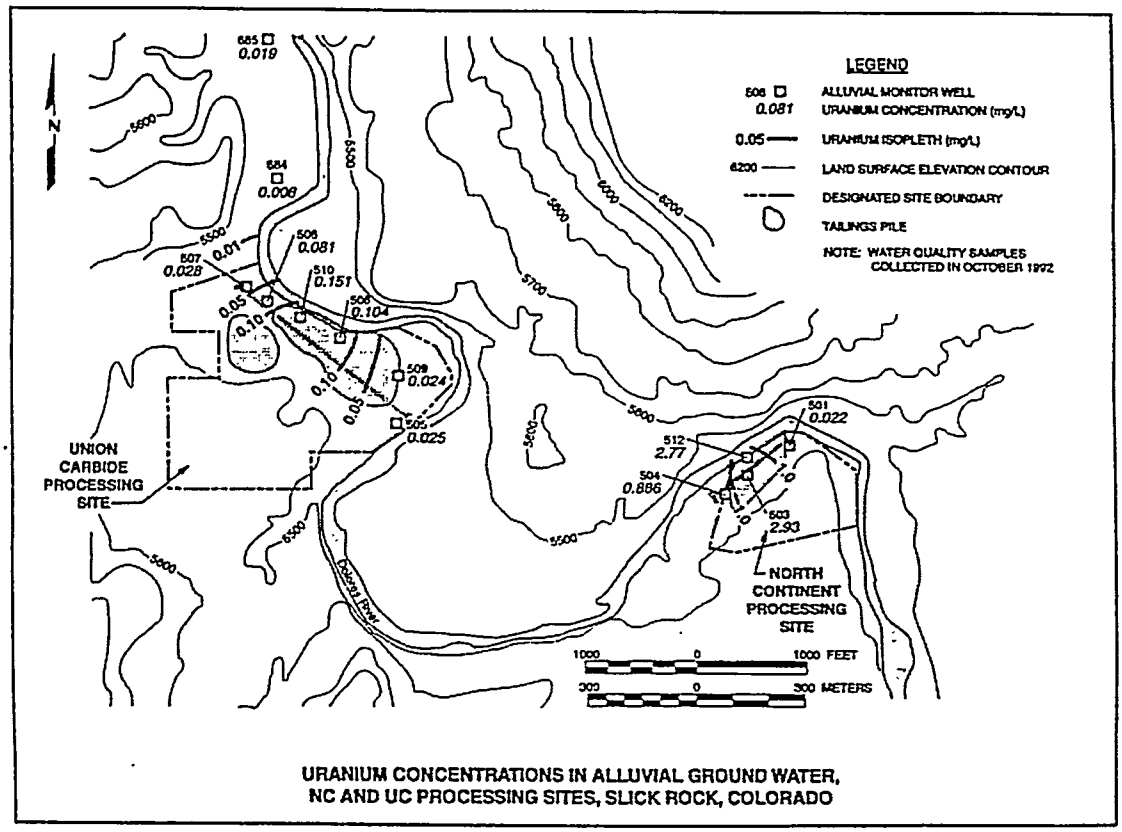

URANIUM CONCENTRATIONS IN ALLUVIAL GROUND WATER, NC AND UC PROCESSING SITES, SLICK ROCK, COLORADO

Figure 11. Slick Rock (Colorado) ^{104} plume. The thick light-gray line is the estimated maximum axial plume length as in figure (see figure 8).

associated with remediation and monitoring. To begin with, these results set very clear limits on what reaction-transport model outputs should look like. Although input functions and sub-models can vary widely because "every site is different", output predictions of U movement in subsurface environments do not exceed roughly 2 kilometers and represent natural plume behavior, unless special chemistries, and possibly hydrologies are involved, e.g., active sulfuric acid leaching or perhaps, demonstrable fast path fractures. Long-term monitoring wells placed ahead of plumes assuming steady long-term plume advance may never detect their targets. *In situ* remediation that relies on mobilization by chelating ligands may ultimately result in anomalous long plume movement. Source term removal alone seems to limit plume advance. This picture assumes no change in the geochemical state of the attenuated uranium near the source, such as the introduction of chelating agents and/or a deleterious shift in redox conditions.

Only two of the few plumes examined for the Title II sites Rio Algom (Utah) and Split Rock (Wyoming) exceed plume lengths >2.5 km, which represent the longest estimated distance in this study. It is expected that Title II sites produce longer plumes because the source term is still in place; however the rest of these fall well within the plume length distribution range (i.e., <2km) obtained for both UMTRA Title I and Title II sites.

Lastly, it should be noted that geochemical factors favor uranium transport to be greater than the transport of many other cationic metals and radionuclides such as Pb, Cd, ^{90}Sr, ^{137}Cs because U is a relatively weak sorber and/or because the soil minerals it forms are relatively soluble. Moreover, the fraction of U that sorbs irreversibly in soils is relatively small. For these reasons, we should expect a plume advance for most other cationic metals and radionuclides to be substantially less than the 2 kilometers observed for U.

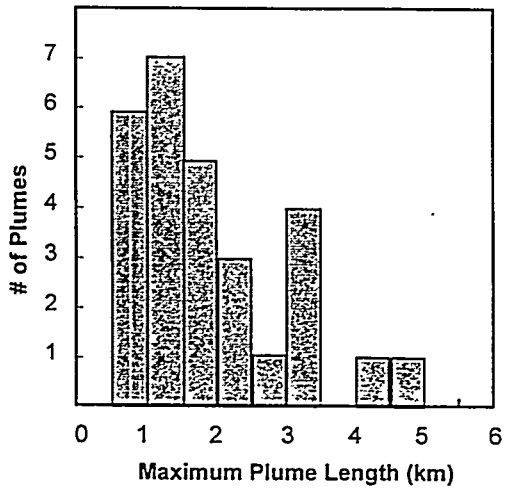

Figure 12. Histogram of maximum plume lengths for all considered U plumes in this study (n=28; see text).

6.0 Acknowledgements

We greatly appreciate the support of the US Nuclear Regulatory Commission (NRC), helpful comments, encouragement, references, and/or plume data from Edward O' Donnell, David W. Rice, Steven C. Golian, James Krumhansl, James A. Davis, Pengchu Zhang, Frank Huang, Bret Leslie, Lauren Goodknight, Ferne C. Allan, Clara Jackson, Kelly Snow, Randolph W. Von Till, Henry Westrich, Randall Cygan, Craig Bethke, and John Ziagos.

References

1. Rice, D.W. et al. UCRL-AR-121762, "Recommendations to improve the cleanup process for California's leaking underground fuel tanks." Lawrence Livermore National Labratory, CA. 1995.

2. Plant, J., Simpson, P.R., Smith, B. and Windley, B.F. *Uranium ore deposits: products of the radioactive Earth.* In *Uranium: mineralogy, geochemistry, and the environment*, P.C. Burns and R. Finch (Editors), Reviews in Mineralogy, Mineralogical Society of America, Washington D. C. 38, 1999.

3. Bethke, C.M. *The Geochemist's Workbench (Release 3.0): A users software guide to Rxn, Act2, Tact, React, and Gtplot.*: Hydrogeology Program, University of Illinois (Urbana-Champaign). 1998.

4. Davis, J.A. NUREG Report Series *in press*, "Surface complexation modeling of uranium(VI) adsorption on natural assemblages." United States Geological Survey (USGS): Menlo Park, CA. 2000.

5. Finch, R. and Murakami, T. *Systematics and paragenesis of uranium minerals.* In *Uranium: mineralogy, geochemistry, and the environment*, P.C. Burns and R. Finch (Editors), Reviews in Mineralogy, Mineralogical Society of America 38, pp. 91-179. 1999.

6. Casas, I. et al. "The role of pe, pH, and carbonate on the solubility of UO2 and uraninite under nominally reducing conditions." *Geochimica et Cosmochimica Acta.* 62, 13: pp. 2223-2231. 1998.

7. Grambow, B. Swedish Nuclear Fuel and Waste Management (SKB) Technical Report 89-13, "Spent fuel dissolution and oxidation: an evaluation of literature data." SKB: Stockholm. 1989.

8. Francis, A.J. "Biotransformation of uranium and other actinides in radioactive wastes." *Journal of Alloys and Compounds.* 271, pp. 78-84. 1998.

9. Suzuki, Y. and Banfield, J.F. *Geomicrobiology of uranium.* In *Uranium: mineralogy, geochemistry, and the environment*, P.C. Burns and R. Finch (Editors), Reviews in Mineralogy, Mineralogical Society of America 38, pp. 394-432. 1999.

10. Huang, F.Y.C., Brady, P.V., Lindgren, E.R. and Guerra, P. "Biodegradation of uranium-citrate complexes: Implications for extraction of uranium from soils." *Environmental Science and Technology.* 32, 3: pp. 379-382. 1998.

11. Abdelouas, A., Lutze, W. and Nuttall, H.E. "Oxidative dissolution of uraninite precipitated on Navajo sandstone." *Journal of Contaminant Hydrology.* 36, 3-4: pp. 353-375. 1999.

12. Abdelouas, A., Lutze, W. and Nuttall, E. "Chemical reactions of uranium in ground water at a mill tailings site." *Journal of Contaminant Hydrology.* 34, 4: pp. 343-361. 1998.

13. Abdelouas, A., Lutze, W. and Nuttall, E.H. *Uranium contamination in the subsurface: characterization and remediation.* In *Uranium: mineralogy, geochemistry, and environment*, P.C. Burns and R. Finch (Editors),

Mineralogical Society of America 38, pp. 433-473. 1999.

14. Kohler, M., Curtis, G.P., Kent, D.B. and Davis, J.A. "Experimental investigation and modeling of uranium(VI) transport under variable chemical conditions." *Water Resources Research.* 32, 12: pp. 3539-3551. 1996.

15. Pabalan, R.T., Turner, D.R., Bertetti, P.F. and Prikryl, J.D. *Uranium(VI) adsorption onto selected mineral surfaces.* In *Adsorption of Metals by Geomedia*, E.A. Jenne (Editor), Academic Press, San Diego. pp. 99-130. 1998.

16. Payne, T.E. and Waite, T.D. NUREG Report Series *in press*, "Uranium(VI) adsorption on ferrihydrate in simple NaNO3/HCO3 systems, and in systems containing additional complexing ligands." United States Geological Survey (USGS): Menlo Park, CA. 2000a.

17. Payne, T.E. and Waite, T.D. NUREG Report Series *in press*, "Uranium(VI) adsorption on kaolinite in simple NaNO3/HCO3 systems, and in systems containing additional complexing ligands." United States Geological Survey (USGS): Menlo Park, CA. 2000b.

18. Tripathi, V.S. "Uranium(VI) transport modeling: Geochemical data and sub-models." Unpublished Ph.D. Thesis, Stanford University, Stanford, CA 1983.

19. Hsi, C.K.D. and Langmuir, D. "Adsorption of uranyl onto ferric oxyhydroxides: application of the surface complexation site-binding model." *Geochimica et Cosmochimica Acta.* 49, 9: pp. 1931-1941. 1985.

20. Redden, G.D., Li, J. and Leckie, J. *Adsorption of U(VI) and citric acid on goethite, gibbsite, and kaolinite.* In *Adsorption of Metals by Geomedia*, E.A. Jenne (Editor), Academic Press, San Diego, CA. pp. 291-315. 1998.

21. Payne, T.E., Lumpkin, G.R. and Waite, T.D. *Uranium(VI) adsorption on model minerals.* In *Adsorption of Metals by Geomedia*, E.V. Jenne (Editor), Academic Press, San Diego. pp. 75-97. 1998.

22. Jenne, E.A. *Adsorption of metals by geomedia: data analysis, modeling, controlling factors, and related issues.* In *Adsorption of Metals by Geomedia*, E.A. Jenne (Editor), Academic Press, San Diego. 1998.

23. Krupka, K.M., Kaplan, D.I., Whelan, G., Serne, R.J. and Mattigod, S.V. EPA 402-R-99-004A&B, "Understanding variation in partition coefficient, Kd, values - Volume II: Review of geochemistry and available Kd values for cadmium, cesium, chromium, lead, plutonium, radon, strontium, thorium, tritium (3H), and uranium." United States of America Environmental Protection Agency (US EPA): Washington, D. C. 1999.

24. Thompson, H.A., Parks, G.A. and Brown, G.E. *Structure and composition of uraniumVI sorption complexes at the kaolinite-water interface.* In *Adsorption of Metals by Geomedia*, E.A. Jenne (Editor), Academic Press, San Diego. pp. 349-399. 1998.

25. Drot, R. and Simoni, E. "Uranium(VI) and europium(III) speciation at the phosphate compounds-solution interface." *Langmuir.* 15, 14: pp. 4820-4827. 1999.

26. Valsami-Jones, E. et al. "The dissolution of apatite in the presence of aqueous metal cations at pH 2-7." *Chem. Geol.* 151, pp. 215-233. 1998.

27. Arey, J.S., Seaman, J.C. and Bertsch, P.M. "Immobilization of uranium in contaminated sediments by hydroxyapatite addition." *Environmental Science and Technology.* 33, 2: pp. 337-342. 1999.

28. Brady, P.V. et al. SAND99-0464, "Site screening and technical guidance for monitored natural attenuation at DOE sites." Sandia National Laboratories: Albuquerque, NM. 1999.

29. Miekeley, N., de jesus, H.C., da Silveira, C.L.P. and Degueldre, C. "Chemical and physical characterization of suspended particles and colloids in waters from the Osamu Utsumi Mine and Morro do Ferro analog study sites, Pocos de Caldas, Brazil." *Journal of Geochemical Exploration.* 45, 1-3: pp. 409-437. 1992.

30. Vilks, P., Cramer, J.J., Shewchuk, T.A. and Larocque, J.P.A. "Colloid and particulate matter studies in the Cigar Lake Natural- Analogue program." *Radiochimica Acta.* 44-5, (pt.2): pp. 305-310. 1988.

31. Vilks, P., Cramer, J.J., Bachinski, D.B., Doern, D.C. and Miller, H.G. "Studies of colloids and suspended particles, Cigar Lake Uranium Deposit, Saskatchewan, Canada." *Applied Geochemistry.* 8, 6: pp. 605-616. 1993.

32. Yanase, N., Payne, T.E. and Sekine, K. "Groundwater geochemistry in the Koongarra Ore deposit , Australia.1. Implications for uranium migration." *Geochemical Journal.* 29, 1: pp. 1-29. 1995a.

33. Environmental Protection Agency (EPA), "Environmental Protection Agency (EPA) - Groundwater Standards for Remedial Actions at Inactive Uranium Processing Sites." *Federal Register*, CFR 40 Part 192. 2866 pp. November, 1995.

34. White, A.F., Delany, J.M., Narasimhan, T.N. and Smith, A. "Groundwater contamination from an inactive uranium mill tailings pile 1. Application of a chemical mixing model." *Water Resources Research.* 20, pp. 1743-1752. 1984.

35. Jacobs Engineering Group Inc. DOE/AL/62350-117 Rev. 0, "UMTRA Project Water Sampling and Analysis Plan: Riverton, Wyoming." Department of Energy (DOE) - Grand Junction Office (GJO): Grand Junction, Colorado. 1994.

36. Jacobs Engineering Group Inc. DOE/AL/6350-122, "UMTRA Project Water Sampling and Analysis Plan: Monument Valley, Arizona." Department of Energy (DOE) - Grand Junction Office (GJO): Grand Junction, Colorado. 1994.

37. Department of Energy (DOE) - Grand Junction Office (GJO), "UMTRA Ground Water Project - F.Y. 1998 Task Order No. 96-5.5." 2000. <http://www.doegjpo.com/gwwp/> (February 2000).

38. Vochten, R. and Van Haverbeke, L. "Transformation of schoepite into the uranyl oxide hydrates : becquerelite, billietite, and wolsendorfite."

Mineralogy and Petrology. 43, 1: pp. 65-72. 1990.

39. Casas, I., Bruno, J., Cera, E., Finch, R.J. and Ewing, R.C. "Characterization and dissolution behavior of a becquerelite from Shinkolobwe, Zaire." *Geochimica et Cosmochimica Acta*. 61, 18: pp. 3879-3884. 1997.

40. Sandino, M.C.A. and Grambow, B. "Solubility Equilibria in the U(Vi)-Ca-K-Cl-H2o System: Transformation of Schoepite Into Becquerelite and Compreignacite." *Radiochimica Acta*. 66-7, pp. 37-43. 1994.

41. Finch, R.J., Cooper, M.A., Hawthorne, F.C. and Ewing, R.C. "The crystal structure of schoepite ; [(UO2)(8)O-2(OH)(12)](H2O)(12)." *Canadian Mineralogist*. 34, (pt.5): pp. 1071-1088. 1996.

42. Sowder, A.G., Clark, S.B. and Fjeld, R.A. "The effect of silica and phosphate on the transformation of schoepite to becquerelite and other uranyl phases." *Radiochimica Acta*. 74, pp. 45-49. 1996.

43. Wronkiewicz, D.J., Bates, J.K., Wolf, S.F. and Buck, E.C. "Ten-year results from unsaturated drip tests with UO2 at 90 degrees C: Implications for the corrosion of spent nuclear fuel." *Journal of Nuclear Materials*. 238, 1: pp. 78-95. 1996.

44. Sowder, A.G., Clark, S.G. and Field, R.A. "The transformation of uranyl oxide hydrates: The effect of dehydration on synthetic metaschoepite and its alteration to becquerelite." *Environmental Science and Technology*. 33, 20: pp. 3550-3555. 1999.

45. Diaz-Arocas, P. and Grambow, B. "Solid-liquid phase equilibria of U(VI) in NaCl solutions." *Geochimica et Cosmochimica Acta*. 62, 2: pp. 245-263. 1998.

46. Department of Energy (DOE) - Grand Junction Office (GJO), "Hanford Tank Farms Vadose Zone Project." 2000. <http://www.doegjpo.com/programs/hanf/HTFVZ.html> (February 2000).

47. Arnett, M.W. and Mamatey, A.R.e. WSRC-TR-00314, "Savannah River Site: Environmental Data for 1998." Westinghouse Savannah River Site Company: Aiken, South Carolina. 1998.

48. Hobday, D.K. and Galloway, W.E. "Groundwater processes and sedimentary uranium deposits." *Hydrogeology Journal*. 7, pp. 127-138. 1999.

49. Min, M.Z., Zhai, J.P. and Fang, C.Q. "Uranium-series radionuclide and element migration around the Sanerliu granite-hosted uranium deposit in southern China as a natural analogue for high-level radwaste repositories." *Chemical Geology*. 144, 3-4: pp. 313-328. 1998.

50. Georgeaniel, B., Leroy, J.L. and Poty, B. "Volcanogenic uranium mineralizations in the Sierra-Pena-Blanca district; Chihuahua, Mexico: 3 genetic models." *Economic Geology and the Bulletin of the Society of Economic Geologists*. 86, 2: pp. 233-248. 1991.

51. Pearcy, E. and Leslie, B. CNWRA 93-01S, "Geochemical Natural Analog Research." NRC High-Level Radioactive Waste Research at CNMRA January-June 1993 Center for Nuclear

Regulatory Analyses: San Antonio, Texas. 1993.

52. Pearcy, E.C., Prikryl, J.D., Murphy, W.M. and Leslie, B.W. "Alteration of uraninite from the Nopal-I Deposit, Pena Blanca district, Chihuahua, Mexico, compared to degradation of spent nuclear-fuel in the proposed United States high-level nuclear waste repository at Yucca Mountain, Nevada." *Applied Geochemistry*. 9, 6: pp. 713-732. 1994.

53. Murphy, W.M. "Natural Analogs for Yucca Mountain." *Radwaste Magazine*. 2, 6: pp. 44-50. 1995.

54. Prikryl, J.D., Pickett, D.A., Murphy, W.M. and Pearcy, E.C. "Migration behavior of naturally occurring radionuclides at the Nopal I uranium deposit, Chihuahua, Mexico." *Journal of Contaminant Hydrology*. 26, 1-4: pp. 61-69. 1997.

55. Proceedings of the 7th Annual International Conference on High Level Waste Management. "Nopal I uranium deposit: A study of radionuclide migration." Las Vegas, Nevada; 43-45. Apr 29-May 3, 1996.

56. High Level Waste Management; Proceedings of the 7th Annual International Conference. "Numerical analysis of a proposed percolation experiment at the Pena Blanca natural analog site." Las Vegas, Nevada; 226-228. April 30 - May 5, 1995.

57. Ahonen, L., Ervanne, H., Jaakkola, T. and Blomqvist, R. "Redox Chemistry in Uranium-Rich Groundwater of Palmottu Uranium Deposit, Finland." *Radiochimica Acta*. 66, 7: pp. 115-121. 1994.

58. Suutarinen, R., Blomqvist, R., Halonen, S. and Jaakkola, T. "Uranium in groundwater in Palmottu analog study site in Finland." *Radiochimica Acta*. 52-3, (pt.2): pp. 373-380. 1991.

59. Linklater, C.M. et al. "A natural analogue of high-pH cement pore waters from the Maqarin area of northern Jordan: Comparison of predicted and observed trace-element chemistry of uranium and selenium." *Journal of Contaminant Hydrology*. 21, 1-4: pp. 59-69. 1996.

60. Smellie, J.A.T., Karlsson, F. and Alexander, W.R. "Natural analogue studies: Present status and performance assessment implications." *Journal of Contaminant Hydrology*. 26, 1-4: pp. 3-17. 1997.

61. Stockman, H., Krumhansl, J., Ho, C. and McConnell, V. NUREG/CR-6221 SAND94-0650, "The Valles Natural Analogue Project." Sandia National Laboratories. 1994.

62. Biehler, D. and Falck, W.E. "Simulation of the effects of geochemical reactions on groundwater quality during planned flooding of the Konigstein uranium mine, Saxony, Germany." *Hydrogeology Journal*. 7, 3: pp. 284-293. 1999.

63. Nitzsche, O. and Merkel, B. "Reactive transport modeling of uranium 238 and radium 226 in groundwater of the Konigstein uranium mine; Germany." *Hydrogeology Journal*. 7, 5: pp. 423-430. 1999.

64. Chapman, N.A., McKinley, I.G., Shea, M.E. and Smellie, J.A.T. "The Pocos de Caldas Project: an introduction and summary of its implications for

radioactive waste disposal." *Journal of Geochemical Exploration.* 45, 1-3: pp. 1-24. 1992.

65. Chapman, N.A., McKinley, I.G., Shea, M.E. and Smellie, J.A.T. *The Pocos de Caldas Project: natural analogues of processes in a radioactive waste repository.*: Elsevier Science Publishers B.V., The Netherlands. 1993.

66. Yanase, N., Payne, T.E. and Sekine, K. "Groundwater geochemistry in the Koongarra Ore deposit; Australia .2. Activity ratios and migration mechanisms of uranium series radionuclides." *Geochemical Journal.* 29, 1: pp. 31-54. 1995b.

67. Curtis, D.B., Benjamin, T.M. and Gancarz, A.J. DOE/TIC-4621 Vol. 1, "The Oklo reactors: Natural analogs to nuclear waste repositories: Technology of high-level nuclear waste disposal. Advances in sciences and engineering of the management of high-level nuclear wastes - volume 1." Los Alamos National Laboratory: Los Alamos, NM. 1981.

68. Ayora, C., Salas, J., Made, B. and Ledoux, E. "Reactive transport around Bangombe uranium deposit, Gabon." *Mineralogical Magazine.* 62A, 1: pp. 87-88. 1998.

69. Edghill, R. "The redistribution of uranium with weathering in the Koongarra uranium deposit." *Radiochimica Acta.* 52-3, (pt.2): pp. 381-386. 1991.

70. Murakami, T., Ohnuki, T., Isobe, H. and Sato, T. "Mobility of uranium during weathering." *American Mineralogist.* 82, 9-10: pp. 888-899. 1997.

71. Sato, T. et al. "Iron nodules scavenging uranium from groundwater." *Environmental Science and Technology.* 31, 10: pp. 2854-2858. 1997.

72. Payne, T.E. DOE/HMIP/RR/92/077, "Alligator Rivers Analogue Project - Groundwater Chemistry." Australian Nuclear Science and Technology Organisation: Menai, Australia. 1992.

73. Townley, L.R. , "Alligator Rivers Analogue Project - Hydrogeological Modelling." Final Report - Vol. 6 DOE/HMIP/RR/92/076 Australian Nuclear Science and Technology Organisation: Menai, Australia. 1992.

74. Toulhoat, P.T. et al. "Preliminary studies of groundwater flow and migration of uranium isotopes around the Oklo natural reactors (Gabon)." *Journal of Contaminant Hydrology.* 21, 1-4: pp. 3-17. 1996.

75. GEOFLUIDS III. "The redox control of groundwater around Okelobondo uranium deposit (Gabon): 1D reactive transport modeling." Barcelona, Spain; *in press.* .

76. Schorscher, H.D. and Shea, M.E. "The regional geology of the Pocos de Caldas alkaline complex: mineralogy and geochemistry of selected nepheline syenites and phonolites." *Journal of Geochemical Exploration.* 45, 1-3: pp. 25-51. 1992.

77. Cathles, L.M. and Shea, M.E. "Near-field high temperature transport: evidence from the genesis of the Osamu Utsumi uranium mine; Pocos de Caldas alkaline complex, Brazil." *Journal of Geochemical Exploration.* 45, 1-3: pp. 565-603. 1992.

78. Waber, N., Schorscher, H.D. and Peters, T. "Hydrothermal and supergene uranium mineralization At the Osamu Utsumi mine, Pocos de Caldas, Minas Gerais, Brazil." *Journal of Geochemical Exploration*. 45, 1-3: pp. 53-112. 1992.

79. Lichtner, P.C. and Waber, N. "Redox front geochemistry and weathering: theory with application to the Osamu Utsumi uranium mine, Pocos de Caldas, Brazil." *Journal of Geochemical Exploration*. 45, 1-3: pp. 521-564. 1992.

80. Read, D. "Geochemical modeling of uranium redistribution in the Osamu Utsumi mine, Pocos de Caldas." *Journal of Geochemical Exploration*. 45, 1-3: pp. 503-520. 1992.

81. Toulhoat, P. and Beaucaire, C. "Geochemistry of waters linked to the Cigar Lake Uranium Deposit (Saskatchewan, Canada) and uses of uranium and lead isotopes in prospecting." *Canadian Journal of Earth Sciences*. 30, 4: pp. 754-763. 1993.

82. International Conference on Radioactive Waste Management. "A natural analog for a fuel waste disposal vault." Winnipeg, Canada; 697-702. 1986.

83. Cramer, J.J. and Smellie, J.A.T. AECL-10851, "Final report of the AECL/SKB Cigar Lake analog study." EACL Research Whiteshell Laboratories. 1994.

84. Curtis, D., Fabryka Martin, J., Dixon, P. and Cramer, J. "Nature's uncommon elements: Plutonium and technetium." *Geochimica et Cosmochimica Acta*. 63, 2: pp. 273-283. 1999.

85. Liu, J.S., Yu, J.W. and Neretnieks, I. "Transport modelling in the natural analogue study of the Cigar Lake uranium deposit (Saskatchewan, Canada)." *Journal of Contaminant Hydrology*. 21, 1-4: pp. 19-34. 1996.

86. Bruno, J., Casas, I., Cera, E. and Duro, L. "Development and application of a model for the long-term alteration of UO2 spent nuclear fuel: Test of equilibrium and kinetic mass transfer models in the Cigar Lake ore deposit." *Journal of Contaminant Hydrology*. 26, 1-4: pp. 19-26. 1997.

87. McNab, W.W.J. et al. UCRL-AR-133361, "Historical case analysis of CVOC plumes." Lawrence Livermore National Laboratories: Livermore, CA. 1999.

88. Jacobs Engineering Group Inc. DOE/AL/62350-95D, "UMTRA Project Water Sampling and Analysis Plan: Canonsburg and Burrell, Pennsylvania." Department of Energy (DOE) - Grand Junction Office (GJO): Grand Junction, Colorado. 1994.

89. Crow-Butte Resources Inc. Nuclear Regulatory Commission (NRC) Public Document - Docket#: 40-8943, "Mine Unit 1 Restoration Report - Crow Butte Uranium Project - Nuclear Regulatory Commission (NRC) Public Document." NRC: Washington D.C. 2000.

90. Department of Energy (DOE) - Grand Junction Office (GJO), "Final site observational work plan for the UMTRA project site at Falls City, Texas." 1997. <http://www.doegjpo.com/gwwp/fct/sowp/> (February 2000).

91. Fluor-Daniel/Fernald. FEMP-2538 Special UC-707, "1996 - Site Environmental Report, U.S. Department of Energy, Fernald Field Office,

Contract #: DE-A24-92OR21972." Environmental Monitoring Project - Fluor Daniel/Fernald. 1997.

92. Jacobs Engineering Group Inc., "UMTRA Project and DOE/GJO Project: Grand Junction, Colorado." 2000. <http://www.doegipo.gov/> (February 2000).

93. Jacobs Engineering Group Inc. DOE/AL/62350-132 Rev. 0, "UMTRA Project Water Sampling and Analysis Plan: Gunnison, Colorado." Department of Energy (DOE) - Grand Junction Office (GJO): Grand Junction, Colorado. 1994.

94. Lindgren, E. Unpublished Report, "Natural attenuation of uranium groundwater plumes at UMTRA sites: A one dimensional analysis of historical data." Sandia National Laboratories: Albuquerque, NM. 1999.

95. Earth and Environmental Technical Services - Westinghouse/Hanford. DOE/RL-96-01 Revision 0 UC-702, "Annual Report for RCRA Groundwater Monitoring Projects at Hanford Site Facilities for 1995." Earth and Environmental Technical Sevices - Westinghouse Hanford Company - Dept. of Energy (DOE). 1996.

96. Kennecott Uranium Company. Nuclear Regulatory Commission (NRC) Public Document - Docket #: 40-8584, "Sweetwater Uranium Project - Annual Corrective Action Program Review for 1999 - Groundwater Monitoring Report - Nuclear Regulatory Commission (NRC) Public Document." NRC: Washington D.C. 2000.

97. Ferry, L. et al. UCRL-AR-132609 DR, "Draft site-wide feasibility study for Lawrence Livermore National Laboratory site 300." Lawrence Livermore National Laboratory, CA. 1999.

98. Jacobs Engineering Group Inc. DOE/AL/62350-125 REV. 0, "UMTRA Project Water Sampling and Analysis Plan: Maybell, Colorado." Department of Energy (DOE) - Grand Junction Office (GJO): Grand Junction, Colorado. 1994.

99. Department of Energy (DOE) - Grand Junction Office (GJO), "UMTRA Project and DOE/GJO Project: Monticello, Colorado." 2000. <http://www.doegipo.gov/> (February 2000).

100. Jacobs Engineering Group Inc. DOE/AL/62350-121F, "UMTRA Project Water Sampling and Analysis Plan: Naturita, Colorado." Department of Energy (DOE) - Grand Junction Office (GJO): Grand Junction, Colorado. 1994.

101. Jacobs Engineering Group Inc. DOE/AL/62350-141 Rev. 0, "UMTRA Project Water Sampling and Analysis Plan: Old and New Rifle, Colorado." Department of Energy (DOE) - Grand Junction Office (GJO): Grand Junction, Colorado. 1994.

102. Rio-Algom Mining Corp. Nuclear Regulatory Commission (NRC) Public Document - Docket#: 40-8084, "Annual Corrective Action Plan Review 1998-1999 - Rio Algom mine - Lisbon Facility." NRC: Washington D.C. 1999.

103. Narasimhan, T.N., White, A.F. and Tokunaga, T. "Groundwater Contamination From an Inactive Uranium Mill Tailings Pile. 2. Application of a Dynamic Mixing

Model." *Water Resources Research.* 22, 13: pp. 1820-1834. 1986.

104. Jacobs Engineering Group Inc. DOE/AL/62350-146 Rev. 0, "UMTRA Project Water Sampling and Analysis Plan: Slick Rock, Colorado." Department of Energy (DOE) - Grand Junction Office (GJO): Grand Junction, Colorado. 1994.

105. Duke-Engineering. Nuclear Regulatory Commision (NRC) Public Document - Docket#: 40-8904, "L-Bar Groundwater Corrective Action Program - 1999 Review Report." NRC: Washington D.C. 1999.

106. Shepherd Miller Inc. Nuclear Regulatory Commission (NRC) Public Document - Docket #: 40-1162, "Western Nuclear Split Rock Mill Site - Site Ground Water Characterization and Evaluation, Appendix F, Geochemical Characterization Report - Nuclear Regulatory Commission (NRC) Public Document." NRC: Washington D.C. 1999.

107. Argonne National Laboratory-Environmental Assessment Division. DOE/OR/21548-569, "Feasibility study for remedial action for the groundwater operable units at the chemical plant area and the ordinance works area at the Weldon Spring Site, Weldon Spring, Missouri." Argonne National Laboratory, Environmental Assessment Division. 1998.

108. Oversby, V.O. and Konsul, V.M.O. SKB-TR-96-14, "Oklo: Des reacteurs nucleaires fossiles (Oklo: The fossil nuclear reactors). Physics study (R Naudet, CEA) - Translation of chapters 6, 13, and conclusions." Swedish Nuclear Fuel and Waste Management (SKB): Stockholm. 1996.

109. Gurban, I., Laaksoharju, M., Ledoux, E., Made, B. and Salignac, A.L. SKB-TR-98-06, "Indications of uranium transport around the reactor zone at Bagombe (Oklo)." Swedish Nuclear Fuel and Waste Management (SKB): Stockolm, Sweden. 1998.

110. Holmes, D.C., Pitty, A.E. and Noy, D.J. SKB Technical Report 90-14, "Geomorphological and hydrogeological features of the Pocos de Caldas caldera, and the Osamu Utsumi mine and Morro do Ferro analogue study sites, Brazil." Swedish Nuclear Fuel and Waste Management (SKB). 1990.

111. Nordstrom, D.K., Smellie, J.A.T. and Wolf, M. SKB Technical Report 90-15, "Chemical and isotopic composition of groundwaters and their seasonal variability at the Osamu Utsumi mine and Morro do Ferro analogue study sites, Pocos de Caldas, Brazil." . 1990.

112. Cross, J.E., Haworth, A., Neretnieks, I., Sharland, S.M. and Tweed, C.J. "Modeling of Redox Front and Uranium Movement in a Uranium-Mine At Pocos de Caldas." *Radiochimica Acta.* 52-3, (pt.2): pp. 445-451. 1991.

113. Chapman, N.A., McKinley, I.G., Shea, M.E. and Smellie, J.A.T. SKB Technical Report 90-24, "The Pocos de Caldas Project: Summary of its implications for radioactive waste management." Swedish Nuclear Fuel and Waste Management (SKB). 1991.

114. Makhijani, A., Hu, H. and Yih, K. (Editors), *Nuclear Wastelands: a global guide to nuclear weapons production and its health and environmental effects.*

MIT Press, Cambridge, Massachusetts 666 pp. 1995.

115. Tailings and Mine Waste 2000 Conference. "Acid In Situ Leach Uranium Mining - 1. USA and Australia." Fort Collins, Colorado; 517-526. January 2000.

116. Tailings and Mine Waste 2000 Conference. "Acid In Situ Leach Uranium Mining - 2. Soviet Block and Asia." Fort Collins, Colorado; 527-536. January 2000.

117. Jacobs Engineering Group Inc. DOE/AL/62350-97D. "UMTRA Project Water Sampling and Analysis Plan: Falls City, Texas." Department of Energy (DOE) - Grand Junction Office (GJO): Grand Junction, Colorado. 1994.

118. Mudd, G. "An Environmental Critique of In Situ Leach Mining: The Case Against Uranium Solution Mining." A Research Report for Friends of the Earth (Fitzroy) with The Australian Conservation Foundation Victoria University of Technology. 1998.